Cyclophosphazene Pendant containing Organic Polymers as Polymer Electrolytes

by
Feroz Khan. A. L.

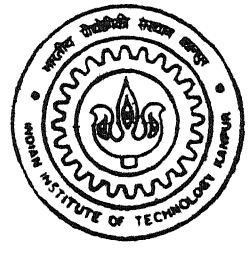

MATERIALS SCIENCE PROGRAMME
INDIAN INSTITUTE OF TECHNOLOGY, KANPUR

February, 2001

Cyclophosphazene Pendant containing Organic Polymers as Polymer Electrolytes

A thesis submitted
in partial fulfillment of the requirements
for the Degree of

Master of Technology

by

Feroz Khan. A. L.

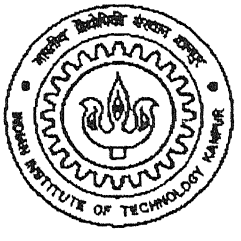

Materials Science Programme
INDIAN INSTITUTE OF TECHNOLOGY KANPUR
February 2001

28.2.01

Certificate

This is to certify that the present work, entitled "**Cyclophosphazene pendant containing organic polymers as polymer electrolytes**" by **Mr. Feroz Khan. A. L (Roll No: 9911205)** has been carried out under our supervision and that this work has not been submitted elsewhere for a degree

Dr. K. Shahi
Professor
Materials Science Programme
Indian Institute of Technology
Kanpur
Date २८ - २ - २००१

Dr. V. Chandrasekhar
Professor
Dept. of Chemistry
Indian Institute of Technology
Kanpur
Date. २८ २ - २००१

Abstract

Polymer electrolytes have attracted considerable attention because of their potential applications in various electrochemical devices, especially high energy density batteries The properties that make them attractive are the (a) easy processability (b) film formability, (c) mechanical flexibility so as to give good contact with the battery electrodes even during charge discharge cycles, (d) light weight, etc A large variety of polymer hosts such as poly(ethylene oxide) (PEO), poly(propylene oxide) (PPO), poly(ethylene amine) (PEI), polyphosphazenes (MEEP), etc , have been employed to develop new ionically conducting polymer-salt complexes The basic feature for a polymer to be a host for metal salts is the concentration of polar groups present in it Although the conventional polymer hosts such as PEO, MEEP, etc , have basic sites, problems arise either in the form of crystalline nature of the polymer (PEO) or the dimensional stability (MEEP) at ambient temperatures

Thus in an attempt to prepare a new polymer electrolyte which is amorphous in nature and at the same time has a good dimensional stability and high concentration of basic sites, an organic polymer with cyclophosphazene pendant groups containing oligoethyleneoxy side-chains, poly(2-[(4′-vinyl-4-biphenylyl)oxy]-2,4,4,6,6-pentakis[2-(2-methoxy ethoxy)ethoxy]cyclotriphosphazene) (PPMEE) was prepared and complexed with sodium iodide in various proportions Five compositions of the polymer-salt complex were prepared and studied The polymer and its complexes were characterized using the various techniques available such as NMR, IR, XRD, Mass and impedance spectroscopy It was found that all the complexes were amorphous in nature and showed good conductivity values (e g. 3 4 x 10^{-6} Ω^{-1} cm^{-1} at 47 °C), higher than that of analogous PEO complexes. The dielectric constant studies revealed the presence of interfacial polarization A new organic polymer with cyclophosphazene pendant groups containing branched oligoethyleneoxy side-chains, poly(2-[(4′-vinyl-biphenylyl)oxy]-2,4,4,6,6-pentakis[2,3-bis(2-(2-methoxy ethoxy)ethoxy)propoxy]cyclotriphosphazene) (PPOMEE) was also prepared and characterized using NMR and Mass techniques such as ^{1}H NMR, 2D COSY, Low temperature NMR, FAB-Mass etc This material was found to be a gel-

like solid and is expected to show very high conductivity values when complexed with metal salts

Chapter 1 in this thesis gives a brief overview of the role played by polymer electrolytes in the field of solid state ionics. Theory of polymer electrolytes is also discussed Chapter 2 details the preparation of the polymers and their characterization using NMR, Mass and IR techniques Chapter 3 is devoted to the synthesis and characterization of the polymer electrolyte complexes. Finally Chapter 4 gives the conclusions and the future scope of the work

Acknowledgements

With great pleasure and respect, I thank Prof K. Shahi and Prof V Chandrasekhar, for introducing me to my dream-field of polymer electrolytes and the exemplary guidance they provided for the past one-year.

I also take this oppurtunity to thank Prof. D C. Agrawal, Prof Jitendra Kumar, Prof Y N. Mohapatra, Prof K N Rai, Prof. D. Gupta who have shared their valuable knowledge with me and increased my calibre of understanding the scientific world.

I thank my teachers Prof Sankaran, Prof Nagarajan, Prof. Santhanam, Prof. Palanichamy who developed in me the interest for this field.

I am grateful to Mr V Krishnan who has guided me throughout the life at IIT Kanpur Without his help I wouldn't have completed my M. Tech course

I thank the technicians, Mr. Nayab Ahmed, Mr. Uma Shankar, Mr Joshi and all non-teaching staff who have helped me in completing my project and during my stay at IIT

I thank my labmates, Senthil Andavar, Nagendran, Kingsley, Athi, Anshuman, Baskar, Boomi, Shanmugam, Ashotosh, Sudha, Manish, Jaiprakash and Anoop for their constant encouragement

Special mention should be made about my friends, Murali, Vijay, Venkatraman without whom life at IIT would not have been a memorable one I also thank my other friends, Pachai, Nagarajan, Anand, Simi, Animesh, Niraj, Sreya and all others who have been with me at some point of time.

I don't have words for Sakthi, Rajesh and J.P.

Last but not the least I owe my gratitude to my parents, Shan, Rizu and Hema. I wouldn't have achieved this feat in my life but for their meticulous care and guidance I dedicate this thesis to them.

I thank CSIR and IIT for the financial support.

Above all, I thank the Almighty, for providing me with this oppurtunity to prove myself in life.

Feroz Khan

Contents

List of Figures

List of Tables

Abbreviations

AAB	4-acetoxy-4′-acetyl biphenyl
a c	Alternating current
CPHVB	2-(4′-vinyl-4-biphenylyloxy)pentachlorocyclotriphosphazene
d c	Direct current
HEB	4-hydroxy-4′-hydroxyethyl biphenyl
HOMEE	2,3-bis(2-(2-methoxy ethoxy)ethoxy)propanol
HVB	4-hydroxy-4′-vinyl biphenyl
MEEP	Poly(2-(2-methoxy ethoxy)ethoxy phosphazene)
MEETS	2-(2-methoxy ethoxy)ethyl *p*-toluenesulphonate
NMR	Nuclear magnetic resonance
PEO	Poly(ethylene oxide)
PMEE	2-[(4′-vinyl-4-biphenylyl)oxy]-2,4,4,6,6-pentakis[2-(2-methoxy ethoxy)ethoxy]cyclotriphosphazene
POMEE	2-[(4′-vinyl-biphenylyl)oxy]-2,4,4,6,6-pentakis[2,3-bis(2-(2-methoxy ethoxy)ethoxy)propoxy)cyclotriphosphazene
PPMEE	Poly(2-[(4′-vinyl-4-biphenylyl)oxy]-2,4,4,6,6-pentakis[2-(2-methoxy ethoxy)ethoxy]cyclotriphosphazene)
PPO	Poly(propylene oxide)
PPOMEE	Poly(2-[(4′-vinyl-biphenylyl)oxy]-2,4,4,6,6-pentakis[2,3-bis(2-(2-methoxy ethoxy)ethoxy)propoxy]cyclotriphosphazene)
IR	Infrared
TBMEE	1-(*tert*-butyloxy)-2,3-bis(2-(2-methoxy ethoxy)ethoxy propane
TBOH	3-*tert*-butoxy-1,2-propanediol
THF	Tetrahydrofuran
V-T-F	Vogel-Tamman-Fulcher
WLF	William-Landel-Ferry
XRD	X-Ray diffraction

Chapter 1

1.1 Introduction

Over the past four decades the progress in technology has increased the demand for lightweight compact electrical power storage devices The power sources used at present hardly satisfy these requirements. As a result, considerable research effort has been directed towards the investigation of such materials, which can meet the present man's comfort Of the various materials known solid electrolytes are turning out to be promising from the application point of view.

1.2 Super Ionic Solids

As early as 1830, Faraday observed charge transport by movement of ions in an electrolytic solution and put forward the Faraday's laws of electrolysis However the interest in solid electrolytes did not bloom until Tubandt and Lorenz[1] observed that solid AgI had ionic conductivity comparable to those of the best conducting liquid electrolytes

at temperatures higher than 400 °C. At the β to α transition in AgI the conductivity increased three orders of magnitude up to $\sigma = 1.3\ \Omega^{-1}\ cm^{-1}$ This investigation gave way to the birth of a class of electrolytes called **superionic conductors** or **fast ion conductors** or **solid electrolytes**

Typically a superionic solid has the following characteristics[2]·

(a) bonding involving the mobile species is ionic,

(b) electrical conductivity is high (10^{-1} to $10^{-4}\ \Omega^{-1}\ cm^{-1}$),

(c) principal charge carriers are ions which means that $t_{ion} \sim 1$,

(d) electronic conductivity is small, $t_e \sim 10^{4}$

The highest conductivity at room temperature obtained so far is for $RbAg_4I$ ($\sigma = 0\ 27\ \Omega^{-1}\ cm^{-1}$)

Solid electrolytes can be further classified depending on the nature of the materials as,

(a) Crystalline ionic conductors

(b) Amorphous solid electrolytes

(c) Composite solid electrolytes

(d) Polymeric solid electrolytes

The disadvantages of the first three classes are,

(a) They attain a high electrical conductivity only above particular temperatures, which are impracticable for many applications.

(b) When used in solid state batteries, there is loss of contact between the electrodes and the electrolyte arising out of dimensional changes of electrodes during charge – discharge cycles[3, 4].

These disadvantages have inspired the search of ionic solids that are flexible and show high conductivity at ambient temperatures These efforts have resulted in a new class of solid electrolytes known as **polymeric electrolytes**.

1.3 Polymer Electrolytes

Peter Wright and coworkers[5] were the first to report the ionic conductivity of a polymer – salt complex, poly(ethylene oxide) (PEO) with alkali metal salts. A few years later Armand suggested the use of poly(ethylene oxide) as a solid electrolyte system for the transport of ions[6]. Since then the interest in the field of polymeric electrolytes has been enormously increasing with new types of polymeric systems involved in research

Some of the important polymers that have been used in the studies of polymer solid electrolytes include -

(a) poly(ethylene oxide)
(b) poly(propylene oxide)
(c) polysiloxanes
(d) polyphosphazenes
(e) polyacrylates
(f) poly(vinyl pyrrolidine)
(g) poly(ethylene succinate)
(h) poly(vinyl alcohol)
(i) poly(ethylene imine)
(j) poly(alkylene sulphides)

Polymers used as hosts in electrolyte systems can be mainly classified into two types·

(a) Linear polymers
(b) Comb-like polymers
(c) Network polymers

1.3.1 Linear Polymers

Linear polymers like PEO, poly(propylene oxide), etc , contain the donor atoms (basic groups) in the main backbone. Of the polymer electrolytes investigated till now, PEO-electrolytes have received much attention. PEO is a semicrystalline material

with about 60% of the bulk being crystalline at room temperature and the remainder being present as an amorphous elastomeric phase. Studies on this system have revealed that the properties of the polymer – salt complex appear to have very little variation with polymer molecular weight once a suitably high molecular weight has been achieved[7]. Hence one can conclude that the polymer motions relevant to ionic conductivity are not the gross backbone diffusion of the polymer backbone but rather the segmental motions, which are independent of molecular weight. Berthier and coworkers demonstrated that ion transport preferentially occurs in the amorphous phase of PEO-salt complexes[8]. Due to the presence of the crystalline domain PEO-electrolytes show low conductivity at room temperature[9] There is also extensive literature on other linear polymers such as poly(propylene oxide)[10], poly(ethylene glycol)[11, 12], poly(ethylene imine)[13], etc ,

1.3.2 Comb-like Polymers

Since the ion transport in polymer electrolytes is due to short segmental motions in the polymer, interest started inclining towards the preparation of amorphous polymers with flexible backbones attached with short chain polar oligomers, which can form complexes with metal salts Allcock and coworkers[14] first reported the synthesis and characterization of polyphosphazene based comb-like polymers They reported that the electrolytes derived from these polymers have conductivity higher upto three orders of magnitude than the corresponding PEO based electrolytes. In comb-like polymers the backbone of the polymer itself does not possess atoms of sufficient basicity to complex the metal ions. However, these polymers possess side chains, which contain the structural features to enable them to function as hosts in polymer electrolytes. Examples of such polymers include polyphosphazenes, polyacrylates, etc. The torsional mobility of polyphosphazenes is inherently much higher than that present in corresponding organic polymers[22]. This backbone conformational flexibility of polyphosphazenes makes it a interesting host for ion transport. The disadvantage of polyphosphazenes is their poor dimensional stability and tendency to undergo viscous flow under pressure Apart from polyphosphazenes other comb like polymers used as hosts are polysiloxane, polyitaconate, etc , which contain short polyether side chains[15 - 18]. Polymethacrylate comb-like polymers which have a less flexible backbone have also been studied[19 - 21]

1.3.3 Network Polymers

Practically, most polymers are inconvenient since they tend to flow at somewhat higher temperatures. Although cells and devices can be designed such that this problem is overcome but this is a serious drawback for potential commercial applications where long-term dimensional stability is required. Cheradame and coworkers[23-25], have reported an extensive series of network polymers, which have better mechanical properties than the linear analogues. These researchers attributed the superior conductivity of the network polymer over the linear polymer to the low degree of crosslinking or the flexible crosslinks employed. Due to such type of crosslinking the segmental motion of the polymer chains is not significantly reduced Although there is a slight reduction in conductivity, crosslinked siloxane and phosphazene comb polymer electrolytes are found to have good mechanical properties[26, 27]. Amorphous materials with high conductivity have also been prepared by radiation crosslinking PEO-salt complexes above their melting point[28].

1.3.4 Formation of a polymer electrolyte

The preparation of polymer electrolytes is brought about by dissolving the polymer and the metal salt separately in a common solvent such as methanol, ethanol, acetonitrile or THF followed by a slow removal of the solvent in vacuum The final step of preparation can be casting the electrolyte into a thin film or using in the bulk form Schlenk techniques or glove box methods have to be used during the whole operation in order to ensure the absence of moisture. The morphology and the ion transport properties of the electrolyte may vary with the choice of the solvent if the polymer-salt complex has partial crystalline nature[7]. The complex forming reaction can be given as,

$$m\mathrm{MX} + (-\mathrm{RY}-)_n \text{ ---------- } (\mathrm{MX})_m\ (-\mathrm{RY}-)_n$$

1.3.3 Network Polymers

Practically, most polymers are inconvenient since they tend to flow at somewhat higher temperatures Although cells and devices can be designed such that this problem is overcome but this is a serious drawback for potential commercial applications where long-term dimensional stability is required. Cheradame and coworkers[23-25], have reported an extensive series of network polymers, which have better mechanical properties than the linear analogues. These researchers attributed the superior conductivity of the network polymer over the linear polymer to the low degree of crosslinking or the flexible crosslinks employed. Due to such type of crosslinking the segmental motion of the polymer chains is not significantly reduced. Although there is a slight reduction in conductivity, crosslinked siloxane and phosphazene comb polymer electrolytes are found to have good mechanical properties[26, 27]. Amorphous materials with high conductivity have also been prepared by radiation crosslinking PEO-salt complexes above their melting point[28].

1.3.4 Formation of a polymer electrolyte

The preparation of polymer electrolytes is brought about by dissolving the polymer and the metal salt separately in a common solvent such as methanol, ethanol, acetonitrile or THF followed by a slow removal of the solvent in vacuum. The final step of preparation can be casting the electrolyte into a thin film or using in the bulk form Schlenk techniques or glove box methods have to be used during the whole operation in order to ensure the absence of moisture. The morphology and the ion transport properties of the electrolyte may vary with the choice of the solvent if the polymer-salt complex has partial crystalline nature[7] The complex forming reaction can be given as,

$$m\mathrm{MX} + (-\mathrm{RY}-)_n \text{ ---------- } (\mathrm{MX})_m\ (-\mathrm{RY}-)_n$$

where (- RY -) denotes the polymer repeat unit. The above reaction will be thermodynamically favourable only if the Gibb's energy of solvation of the salt by the polymer is more than enough to overcome the lattice energy of the metal salt.

Table 1.1[7] shows the tendency of various salts to form complexes with PEO Those that do not form have very high lattice energy values.

Table 1.1 Salts that form complexes with PEO (ref. 7)

Cation/ Anion	Li^+	Na^+	K^+	Rb^+	Cs^+
F^-	No 1036	No 923	No 821	No 785	No 740
Cl^-	Yes 853	No 786	No 715	No 689	No 659
Br^-	Yes 807	Yes 747	No 682	No 660	No 631
I^-	Yes 757	Yes 704	Yes 644	Yes 630	Yes 604
SCN^-	Yes 807	Yes 682	Yes 619	Yes 616	Yes 568
$CF_3SO_3^-$	Yes 725	Yes 650	Yes 605	Yes 585	Yes 550

**The numbers reported are the lattice energy values of the salts in kJ/mol*

In addition to lattice energy considerations other criteria, which augment the possibility of forming complexes are[7].

(a) High concentration of polar (basic) groups on the polymer chain

(b) The cohesive energy of the polymer needs to be low and its flexibility should be quite high (glass transition temperature, T_g, should be low). This helps in the reorientation of the local coordination geometry to achieve effective solvation.

Most of the polymer electrolytes studied till now are based on oxygen containing monomers Some systems based on N containing monomers such as poly(ethylene imine) and S containing monomers such as poly(alkylene sulphides) have also been studied[7]

1.4 Effect of composition on Conductivity

Polymer electrolytes can be grouped into three main categories on the basis of the changes in conductivity due to change in concentration of the salt

(a) Systems which exhibit no maximum or minimum but a monotonically increasing conductivity as the salt concentration in the complex increases

(b) Systems which show a single maximum in the conductivity versus composition isotherms.

(c) Systems that show a pair of maxima separated by a minimum

A number of polymer salt systems show (a) type of behaviour. The data is presented by a plot of log σ vs log X and the slope in most cases is unity (e.g ,) PEO_{1050}·$LiClO_4$ and in some cases such as PPO-$NaB(C_6H_5)_4$ greater than unity[29 - 31]. A representative figure of this type is given in **Figure 1.1**.

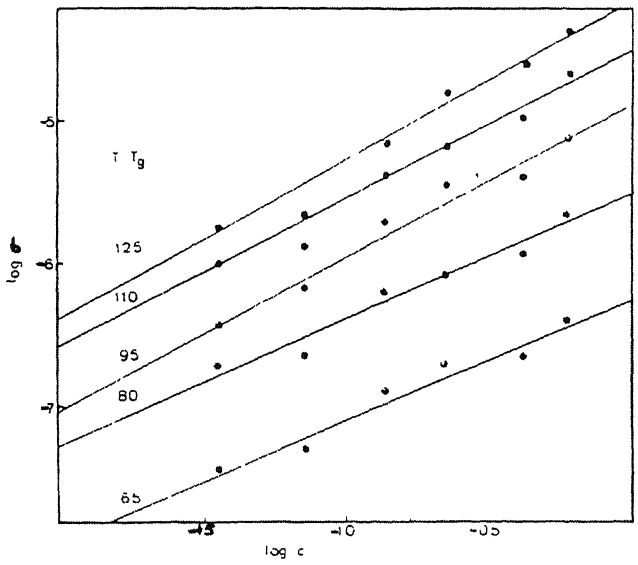

Figure 1.1 log-log plots of ionic conductivity vs. salt concentration for PEO-$NaB(C_6H_5)_4$ (ref. 39)

In the second class the conductivity increases initially, attains a maximum value and then decreases as the salt concentration in the polymer increases[32-35] **Figure 1.2**

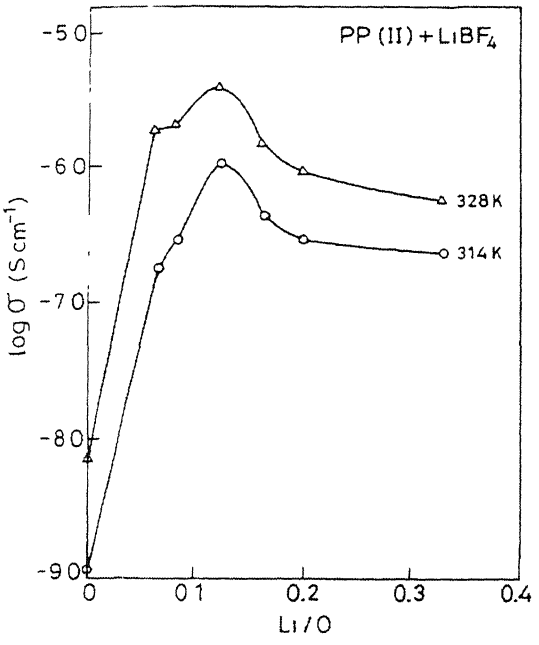

Figure 1.2 log σ vs. Li / O ratio for for PP(II)-$LiBF_4$ (ref 38)

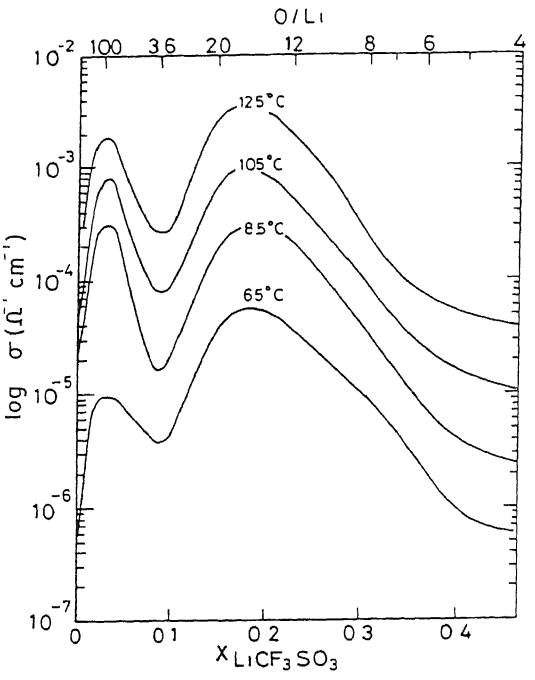

Figure 1.3 log σ as a function of salt concentration for PEO-$LiCF_3SO_3$ (ref 64)

shows this type of behaviour

In the third category, the conductivity vs composition is conspicuous by the presence of a pair of maxima separated by a minimum It is also seen that in such materials the first maximum is less than the second one. **Figure 1.3** shows a polymer electrolyte showing this type of behaviour. There are also other types of behaviour shown by various other polymer salt systems which have been studied[36, 37].

1.5 Effect of temperature on conductivity

In general, the electrical conductivity of solid electrolytes varies with temperature according to the Arrhenius equation,

$$\sigma = \sigma_o \exp\left[\frac{-E_a}{kT}\right] \qquad (1\ 1)$$

However, for most polymeric electrolytes the variation of conductivity with temperature follows the Vogel-Tamman-Fulcher (V-T-F) equation,

$$\sigma = A' T^{-1/2} \exp\left[\frac{-E_a}{kT}\right] \qquad (1.2)$$

Thus a plot of $[\ln (\sigma T^{1/2} / A')]^{-1}$ versus temperature (T) is found to be linear for polymeric electrolytes The pre-exponential factor A' is proportional to the carrier concentration **Figure 1.4** shows this. Armand *et al,* were the first to conclude this after their studies on ((PEO)$_n$ (LiSCN)) and ((PEO)$_n$ (CsSCN))[6].

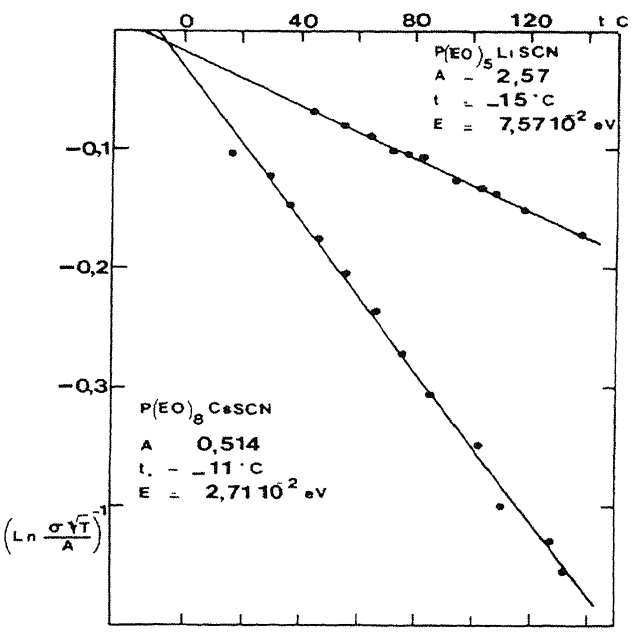

Figure 1.4 Linearization of conductivity plots for PEO-LiSCN and PEO-CsSCN showing the determination of V-T-F parameters (ref 6)

Thus generally speaking, the σ vs. T behaviour of polymer-metal salt complexes may be described by any of the following types[39].

(a) V-T-F behaviour throughout the temperature ranges available

(b) Arrhenius behaviour at lower temperatures and V-T-F behaviour at higher temperatures.

(c) Arrhenius behaviour throughout, but with two different activation energies, high E_a close to T_g and a smaller E_a at higher temperatures

(d) V-T-F behaviour in the temperature ranges slightly above T_g, but Arrhenius behaviour at higher temperatures[40].

(e) Behaviour which is very unlike either Arrhenius or V-T-F at all temperatures

Most polymer electrolytes are found to follow (a), (b) and / or (c) $(PEO)_{45}(LiBr)$ has been found to follow (e) but no proper explanation has been given for such a type of behaviour

The characteristic of most polymer electrolytes to follow V-T-F behaviour can be understood from the concept of the glassy state of a polymer.

1.6 Glassy state

The glassy state of a polymer is characterized by the changes, which occur during the cooling of the polymer at constant pressure As we cool a polymer from its melt viscosity increases When a viscosity of about 10^{15} poises is reached, the rate of intermolecular rearrangement becomes very slow compared to the time scale of cooling Then such a polymer is said to have attained a glassy state and the temperature at which this occurs is called glass transition temperature (T_g), which is usually not well defined In the temperature range of glass transition, the properties of the melt change in a characteristic manner The process is illustrated in **Figure 1.5**. If, as in a crystalline polymer, crystallization occurs then at the melting temperature, there is a discontinuous change, nearly always a fall, in specific volume (Curve ABD). On the other hand, if the melt is cooled and crystallization is prevented, there begins at point E the transition from a highly viscous supercooled melt to a rigid glass At point F the solidification process is complete and a glassy state is formed This is the case for a completely amorphous polymer, for which T_g is somewhat well defined. For partially crystalline polymers, the

change in specific volume with temperature follows the path ABE''F'', i e , the presence of both a melting transition at E'' and a glass transition between E'' and F''.

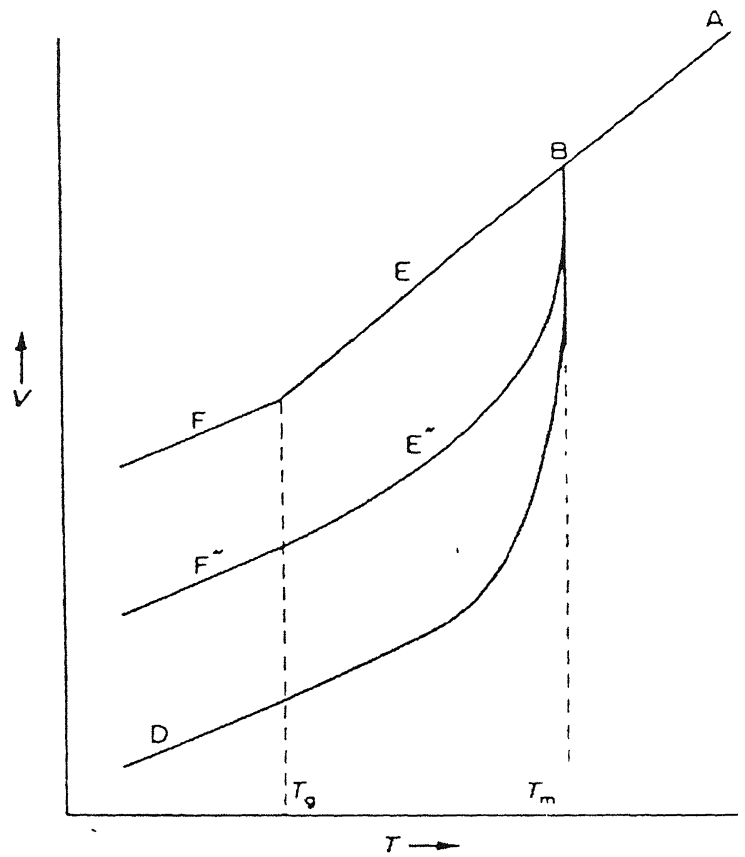

Figure 1.5 Glass transition in polymers

Since the glass transition temperature (T_g) is marked by very rapid increase in viscosity of the polymer melt, the factors considering the polymer viscosity must be taken into consideration For this many empirical relations have been proposed and these have been extended to explain the conduction process in polymer electrolytes.

1.6.1 Free Volume Model

Doolittle and coworkers[41] gave a semi-empirical treatment relating viscosity (η) with volume (V) after studies on n-paraffins,

$$\eta = C\exp\left(\frac{BV_o}{V - V_o}\right) \qquad (1.3)$$

where C is a constant, B also a constant derived from van der Waal's equation and V_o, the theoretical volume of closest packing at 0 K, which was obtained by extrapolating the density data for n-paraffins at 0 K. Equation (1.3) was valid only at high temperatures and high volumes Doolittle defined free volume, V_F as,

$$V_F = (V_T - V_o) \qquad (1.4)$$

Where V_T is the volume of the liquid at any temperature, T.

Cohen and Turnbull[42] derived an equation similar to that of Doolittle's based on the molecular processes occurring by the movement of molecules into voids (formed by the redistribution of free volume). These voids have a size greater than a critical value The contribution of a molecule with a thermal velocity, 'u', to the diffusion coefficient is given by,

$$D(V) = ga(V)u \qquad (1.5)$$

Where 'g' is a geometric factor and $a(V)$ is roughly the diameter of the cage This diffusion coefficient will be zero unless V exceeds a critical value V^* and becomes just large enough to permit another molecule to jump in. So,

$$D = \int_{V^*}^{\infty} D(V)p(V)d(V) \qquad (1.6)$$

Where $p(V)$ is the probability of observing the free volume, V The final expression for diffusion thus obtained is,

$$D = ga^* u\exp\left(\frac{-\gamma V^*}{V_F}\right) \qquad (1.7)$$

Where γ is a Lagrange parameter, a constant close to unity, V^* is near to the molecular volume and a^* is roughly the molecular diameter. From the kinetic theory of gases,

$$u = \sqrt{\frac{8kT}{\pi m}} \qquad (1.8)$$

Since the free volume is considered to be zero at a temperature T_o, V_f is defined slightly differently as,

$$V_F = \alpha V_m (T - T_o) - \beta V_p P \qquad (1\ 9)$$

where α is the coefficient of thermal expansion, β the compressibility and V_m and V_p are the mean molecular volume for the temperature and pressure increment Substituting for V_f in equation (1.7), in the absence of pressure we get,

$$D = ga * u \exp\left[\frac{-\gamma V *}{\alpha V_m (T - T_o)}\right] \qquad (1.10)$$

Taking $u \sim T^{1/2}$, we obtain,

$$D = C_1 T^{1/2} \exp\left[\frac{-B}{T - T_o}\right] \qquad (1\ 11)$$

Where C_1 is a constant and $B = -\gamma V */V_m \alpha$

Using Nernst-Einstein equation,

$$\sigma = \frac{nq^2}{kT} D \qquad (1\ 12)$$

the result obtained is,

$$\sigma = \sigma_o \exp\left(\frac{-B}{T - T_0}\right) \qquad (1\ 13)$$

which is the V-T-F equation with $\sigma \propto T^{-1/2}$.

Although the free volume model is not suitable for discussion of ion transport (for reasons discussed in the forthcoming sections), it is the simplest way to understand the polymer segment mobility. According to this model, as temperature increases, the expansivity of the material produces local empty space, which can accommodate ionic carriers, solvated molecules or even in which polymer segments can themselves move[7]

1.6.2 William-Landel-Ferry approach

The free volume model applies well to liquids Several shortcomings of this model in the context of ionic motion polymer electrolytes have been pointed out For example, free volume model gives incorrect quantitative predictions on the pressure dependence of transport properties[43]. In the case of polymers it is not possible to measure viscosities at high volumes since degradation occurs before the relative free volume, $((V - V_o)/V)$, reaches values above 0 25.

The Williams-Landel-Ferry (WLF) model[44] not only concerns with the viscosity, but also with the relaxation processes which characterize any glass forming material The relationship is given as,

$$\log\left[\frac{\eta(T)}{\eta(T_s)}\right] = \log a_T = \frac{-C_1(T - T_s)}{C_2 + (T - T_s)} \qquad (1\ 14)$$

where C_1 and C_2 are universal constants, T_s is an arbitrary reference temperature and a_T is called the mechanical shift factor. a_T represents the temperature variation of the segmental friction coefficient for any mechanical relaxation. If the WLF relation is coupled with the Stokes-Einstein relationship,

$$D = \frac{kT}{6\pi\eta r_i} \qquad (1\ 15)$$

where D is the diffusion coefficient and r_i is the radius, and the Nernst-Einstein relationship, equation (1.12), then one can write the temperature dependence of conductivity in the WLF form as,

$$\log\frac{\sigma(T)}{\sigma(T_s)} = \frac{C_1(T - T_s)}{C_2 + (T - T_s)} \qquad (1\ 16)$$

The WLF relationship, equation (1 14) is in fact originally based on the empirical V-T-F form, equation (1 2), but written for the viscosity rather than for conductivity. Comparing equation (1 16) and the V-T-F equation,

$$C_2 = T_s - T_o \qquad (1.17)$$

and

$$C_1 = B / k(T_s - T_o) \qquad (1\ 18)$$

These values of C_1 and C_2 can be used to determine the mechanical shift factor, a_T In their original paper, William, Landel and Ferry showed that if instead of T_s, the glass

transition temperature, T_g was substituted the following universal relation can be obtained,

$$\ln a_f = \frac{-17.44(T - T_g)}{51.6 + (T - T_g)} \qquad (1.19)$$

which they claimed to be generally representative of the relaxation or viscosity behaviour of polymers and other glasses in the temperature range $T_g < T < (T_g + 100)$

1.6.3 Configurational Entropy Model

The prediction of WLF approach is often found to be invalid and large deviation from the values of C_1 and C_2 are observed for experimental results. Even more, the free volume cannot be associated with a real molecular volume in the case of polymers but has to be interpreted in terms of inter-intramolecular interactions as well as topology of molecular packing in the amorphous phase These discrepancies in the above discussed theories led to the proposal of Configurational Entropy Model by Gibb's and coworkers[45,46]. This model, based on considerations of entropy fluctuations rather than volume fluctuations, leads to transport properties in agreement with the empirical V-T-F equation (1.2) or WLF equation (1.16). It also predicts pressure dependences and provides a satisfying description of T_o as the temperature at which the excess configurational entropy vanishes. According to Gibbs and DiMarzio, at the glass transition temperature, T_g the molecular relaxation times are too long to permit establishment of equilibrium in the duration of even the slowest experiment. This sluggish relaxation behaviour governing T_g is due to very small number of configurations available to the system at that moment. They gave the transition probabilities for glass-forming liquids in terms of the equilibrium distribution of an isothermal-isobaric ensemble of small systems of the size of a cooperatively rearranging region, which can undergo a transition to a new configuration without a simultaneous configurational change on and outside the boundary.

Adams and Gibbs assumed the number of molecules in the cooperatively rearranging region to be 'z', out of which 'n' have an energy which allow a rearrangement and $(N - n)$ have an energy that do not allow such a transition Then the isothermal-isobaric partition function for the ensemble is given by,

$$\Delta(z,P,T) = \Sigma w(z,E,V) \exp\frac{E_{\alpha}}{kT} \exp\frac{-PV}{kT} \qquad (1.20)$$

where w is the degeneracy of the energy level, E and volume, V of a subsystem. Summing over values of E and V that permit transition, we get a partition function $\Delta'(z, P, T)$ with a Gibb's free energy,

$$G' = z\mu' = -kT \ln \Delta' \qquad (1.21)$$

The fraction of subsystems that permit rearrangement is given by,

$$\frac{N}{n} = \frac{\Delta'}{\Delta} = \exp-\left[\frac{G'-G}{kT}\right] \qquad (1.22)$$

where $G = z\,\mu = -kT \ln \Delta$, is the Gibb's free energy for the whole system and μ and μ' are the chemical potentials of each molecule The cooperative transition probability $W(T)$, is proportional to (n / N) Then by using the relation,

$$z\delta\mu = z(\mu'-\mu) = G'-G \qquad (1.23)$$

we get,

$$W(T) = A \exp\left(\frac{-z\Delta\mu}{kT}\right) \qquad (1.24)$$

Summing up all non-zero values of W(T) we arrive at an average transition probability,

$$W(T)^* = \Sigma A\left[\exp\left(\frac{-\Delta\mu}{kT}\right)\right]^z \qquad (1.25)$$

The summation of this truncated geometric progression gives,

$$W(T)^* = \frac{A}{1-\exp(-\Delta\mu/kT)} \exp\left(\frac{-z^*\Delta\mu}{kT}\right) \qquad (1.26)$$

where z^* is the critical size of the cooperative regions that can undergo transition Since [1- exp (-$\Delta\,\mu$ / kT)] tends to unity, it may be absorbed into the pre-exponential factor giving,

$$W(T)^* = A^* \exp\left(\frac{-z^*\Delta\mu}{kT}\right) \qquad (1.27)$$

In the above equation the temperature dependence of z^* needs to be determined This is determined as follows.

ntropy of the supersystem is given by,

(1.28)

If the supersystem consists of N subsystems then $S_c = N s_c$, where s_c is the configurational entropy of a subsystem of 'z' monomer units If we consider the supersystem to contain Avogadro number (N_1) of segments, then,

$$S_c = k \ln\left[(W_c)^{z/N_1}\right] \qquad (1\ 29)$$

This equation shows that for a given temperature and pressure the configurational entropy of a subsystem increases monotonically with the size of the subsystem, z^* Thus a critical configurational entropy which is characteristic of a representative cooperatively rearranging region can be given by,

$$s_c^* = k \ln\left[(W_c)^{z^*/N_1}\right] \qquad (1.30)$$

Comparing equations (1.29) and (1 30), we get,

$$z^* = \frac{N_1 s_c^*}{s_c} \qquad (1\ 31)$$

Inserting this relation in equation (1 27),

$$W(T)^* = A^* \exp\left(\frac{-\Delta\mu s_c^*}{kTs_c}\right) \qquad (1.32)$$

At temperature, T, the entropy of a system going from glassy to liquid state is related to the specific heat of the system by the relation,

$$S_c(T) = \int \frac{\Delta C_p}{T} dT \qquad (1.33)$$

Where $\Delta C_p = B / T$, is the change in specific heat at temperature, T. B is a constant

$$S_c(T) = \int (B/T^2) dT = B\left(\frac{1}{T_o} - \frac{1}{T}\right) \qquad (1.34)$$

T_o is the glass transition temperature at which the configurational entropy tends to zero Substitution of this equation in equation (1 32) leads to the empirical V-T-F type of equation for the transition probability,

$$W(T)^* = A^* \exp\left[\frac{(-E_a / k)}{T - T_o}\right] \qquad (1.35)$$

where $E_a = \Delta\mu s_c^* T_g / B$ is the apparent activation energy for the polymer rearrangement Ratner emphasized that the above equation describes the motion of the polymer host in the polymer – salt complex and not the ions[39]. However since the jump frequency of the

ions is proportional to the fluidity or transition probability, the above equation can be used in combination with the dynamic band percolation model[39, 47, 48] to obtain an empirical VTF like expression for the conductivity,

$$\sigma = A' T^{-1/2} \exp\left[\frac{(-E_a / k)}{T - T_o}\right] \qquad (1\ 36)$$

where A' is a constant.

In their review, Shriver and Ratner[7] have pointed out the fact that the configurational entropy model is quasi-thermodynamic rather than microscopic, which remains a disadvantage in the sense that no microscopic mechanisms or equation-of-motion pictures are available

1.7 Characterization techniques for polymer electrolytes

Many characteristics of these conducting solid phases formed by the dissociation of salts by ion coordinating macromolecules are still mysteries, eventhough considerable amount of information have been obtained for some systems. Various techniques such as X-Ray diffraction, Infrared & Nuclear Magnetic Resonance spectroscopies, Extended X-Ray Absorption Fine structure, Impedance analysis, etc., have been employed to study the structure and properties of these materials The main objective of these studies is to understand the structure and relate it to the behaviour particularly in terms of ionic conductivity Most of the experiments have been carried out on PEO-metal salt complexes Other systems still need to be explored.

1.7.1 X-Ray Diffraction (XRD)

Single crystal XRD patterns of polymer electrolytes are generally very poor because of the difficulty of obtaining single crystals. However attempts have been made to elucidate structures of some PEO complexes, $PEO_4.HgCl_2$[49], PEO NaI[50], etc ,. Powder XRD has proved to be a better technique for resolving structures of polymer electrolytes for determining structures. Some of the information obtained on PEO-metal salt complexes is given in **Table 1.2**. Various information such as the polymer conformation, coordination number of the cations, bond angles, bond distances, etc , can be extracted from the XRD data Phase changes can also be monitored from XRD patterns[13, 57]

However for amorphous systems XRD patterns are of very little help except that the amorphous nature of the material can be confirmed

Table 1.2 Crystallographic parameters for some PEO-Metal salt complexes

PEO-Metal Salt	Space Group	Cell Dimensions (a, b, c in A^0, β in °)	Reference
$(PEO)_3$ NaI	P $2_1/a$	a = 18.15; b = 7.98; c = 8.41; β = 122.3	50
$(PEO)_4$ NH_4SCN	C 2/c	a = 25.512(3); b = 8.0813(1); c = 16.097(1), β = 125.98(1)	51
$(PEO)_4$.KSCN	C 2/c	a = 25.663(2); b = 8 231(7); c = 15 801(1); β = 125.26(1)	51

1.7.2 Infrared Spectroscopy (IR)

The Infrared (IR) studies on polymer-salt complexes generally give three types of information,

(i) Polymer chain conformation

(ii) Interactions of ions with the polymer

(iii) Ion-ion interactions.

IR studies on PEO-based systems have led to various conclusions on the structure of these complexes. Davidson suggested a gauche conformation[52] Shriver and coworkers coassigned a gauche configuration for the -O-CH_2CH_2-O- group by the assignment of bands in the 800 – 1000 cm^{-1} region[53]. Studies for the evidences on cation – polymer interaction have also been done The C-O-C stretch (1150 cm^{-1}) observed in PEO broadens and also moves to lower frequencies depending on the cation used for complexation IR studies on other polyether – based systems also show similar shifts[12]. More recently, researchers have also been able to assign the various bands obtained for intramolecular modes and related those modes with the local structure and ionic interactions in PEO and other polymer-based systems[54, 55].

1.7.3 Nuclear Magnetic Resonance Spectroscopy (NMR)

Solid State NMR studies have been extensively used to probe the structure and dynamics of polymer electrolytes These studies can be classified as follows,

(i) Studies leading to determination of concentration of amorphous phase

(ii) Relaxation and linewidth studies

(iii) Imaging

(i) Studies leading to determination of concentration of amorphous phase:

NMR allows distinguishing nuclei of the crystalline and the amorphous phase This is based on the determination of spin-spin relaxation time, $\mathbf{T_2}$, which is measure of how fast a nuclear magnetization vector perpendicular to the external magnetic field will decay due to interactions between the spins. This decay time differs for nuclei in different environments due to fluctuating local magnetic fields at the nuclear site It has been shown for PEO-$LiCF_3SO_3$ that by increasing the temperature, the crystalline phase progressively dissolves in the amorphous phase[56]. The nuclei in the amorphous phase take a longer time to decay than nuclei in the crystalline phase.

(ii) Relaxation and Linewidth studies·

Because of the complex structure of polymer electrolytes the relaxation and linewidth studies are difficult to interpret in these cases. Qualitative conclusions have however been made. ^7Li NMR studies in $(PEO)_8$ $LiClO_4$ + x wt % γ-$LiAlO_2$ lead to the conclusion that the local dynamics of the Li-ions is not changed by the addition of γ-$LiAlO_2$ filler[58]. The increase in conductivity observed with the addition of the filler may be caused by the stabilizing and increasing fraction of the amorphous phase. Recently ionic conduction mechanisms in polyphosphazene solids have been studied using ^{13}C, ^{31}P and ^{15}N NMR spectroscopy[59]. The extent of interaction of different cations and the bonding atoms in the polymer backbone have been identified

(iii) Imaging

The NMR imaging technique utilizes the fact that the position of a magnetic nucleus in a magnetic field gradient is encoded onto the NMR frequency By scanning various frequencies of a sample one, two and three-dimensional NMR images

can be obtained[60] Recently water absorption by polymer electrolytes has been studied by NMR imaging[61]

1.7.4 Impedance Analysis

Due to polarization at the electrode-electrolyte interface d c conductance cannot be measured from d c measurements. Therefore ac measurements are generally carried out in order to obtain the complex impedance from which dc conductivity is obtained. There are essentially two a.c methods, one in which the frequency of the a c signal is maintained at a constant value and a d.c. ramp is applied to the cell and the other in which impedance is measured as a function of the frequency of the applied signal over a wide frequency range The second method is of more interest for polymer electrolytes Ideally, there can be two types of polymer electrolytes,

(i) in which only one ionic species is mobile

(ii) in which both the cations and anions of a dissolved salt are mobile

A typical a.c. experiment consists of determining the complex impedance of a cell as a function of the signal frequency and presenting the results in the form of a complex impedance plot In an a c. experiment a sinusoidal voltage is applied to the cell and the sinusoidal current passing through the cell as a result of this perturbation is determined Two parameters are required to relate the current flowing to the applied potential. One is the opposition to the flow of charge, V_o / I_o, which is analogous to the resistance in d c measurements and other is the parameter, θ, which is the phase difference between the voltage and the current. The combination these parameters give the impedance, Z, of the cell Thus for a sinusoidal a c signal given by,

$$v(t) = V_o \exp(j\omega t) \qquad (1.37)$$

applied to a solid electrolyte, the resulting current is given by,

$$i(t) = I_o \exp(j\omega t + \theta) \qquad (1.38)$$

where V_o and I_o are amplitudes of the applied voltage and the resulting current respectively ω is the frequency and $j = \sqrt{-1}$. The complex impedance will then be given by,

$$Z^* = Z \exp(j\omega t) \qquad (1.39)$$

$$= Z\cos\theta + jZ\sin\theta \qquad (1\ 40)$$

or $$Z^* = Z' + jZ'' \qquad (1\ 41)$$

with $$Z = (Z'^2 + Z''^2)^{1/2} \qquad (1\ 42)$$

and $$\tan\theta = \frac{Z''}{Z'} \qquad (1\ 43)$$

The results of an a c experiment can also be presented in dielectric related terms The dielectric constant or permittivity, ε^*, is given by,

$$\varepsilon^* = \varepsilon' - j\varepsilon'' \qquad (1\ 44)$$

with $$\varepsilon' = \frac{\sin\theta}{\omega C_o Z} \qquad (1\ 45)$$

and $$\varepsilon'' = \frac{\cos\theta}{\omega C_o Z} \qquad (1\ 46)$$

C_o is the vacuum permittivity for the distance between the electrodes.

Dielectric loss is defined by,

$$\tan\delta = \frac{\varepsilon''}{\varepsilon'} \qquad (1\ 47)$$

which can be written in terms of the impedance as,

$$\tan\delta = \frac{Z'}{Z''} \qquad (1\ 48)$$

Experimentally the impedance of a cell containing the solid polymer electrolyte and the electrodes is measured The interpretation of results of an a c. experiment relies on finding the equivalent circuit which models the impedance data and extracting values for the individual components which may then be related to the fundamental electrical properties of the cell. The resistors and capacitors are by far the most common components required for modelling electrochemical cells. While analyzing a given system the following combinations of resistors and capacitors are possible.

Purely resistive

A sinusoidal voltage applied across a resistor is always in phase with the current passing through it ($\theta = 0$) and the magnitude of the impedance is simply given by the resistance

i e , $Z' = R$ and $Z'' = 0$

The impedance is independent of frequency. Such a case is represented in the complex plane by a point at a distance, R along the real axis. This is shown in **Figure 1.6(a)**

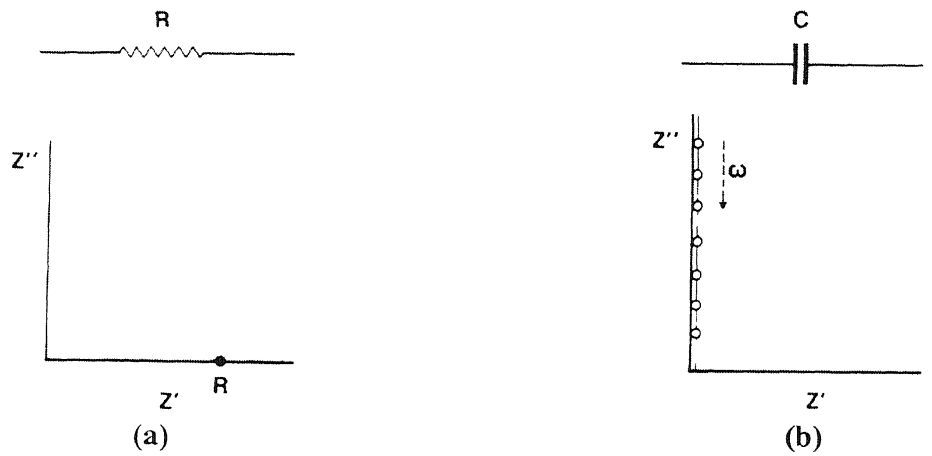

Figure 1.6 Representation of (a) resistor, R. and (b) capacitor, C, in the complex impedance plane (ref 62)

Purely capacitive.

For a purely capacitive system, the voltage lags behind the current by 90° ($\theta = -\pi/2$). The magnitude of the impedance is now frequency-dependent

i e., $Z' = 0$ and $Z'' = -1 / \omega C$

Thus high frequencies or large capacitances give rise to low impedances. We get a vertical line coincident with the imaginary axis in the complex impedance plot. This is represented in **Figure 1.6(b)**.

Resistor and capacitor in series·

When the assembly of the electrodes and the electrolyte behave like a series combination of resistor and capacitor, the total impedance is given by,

$$Z^* = R - \frac{J}{\omega C} \qquad (1.49),$$

which is just the sum of the individual impedances of the components The real part is given by, $Z' = R$ and the imaginary part by, $Z'' = -1 / \omega C$. In the complex impedance plane this defines a vertical line displaced by a distance R along the real axis The complex impedance plot for this is shown in **Figure 1.7(a)**

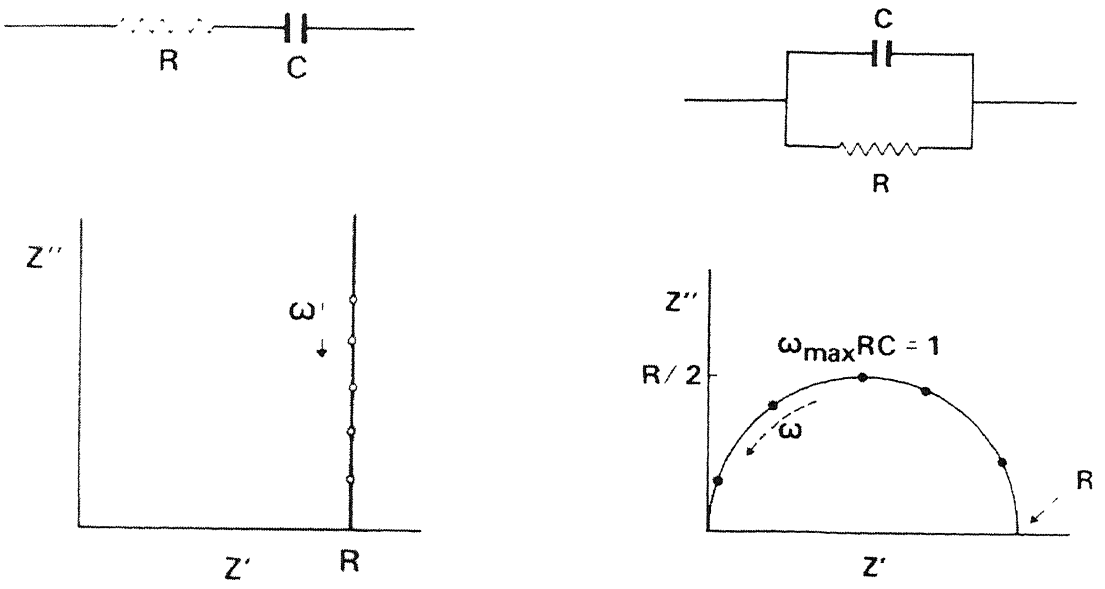

Figure 1.7 Complex impedance plots for a combination of a resistor, R, and capacitor, C, (a) in series and (b) in parallel (ref 62)

Resistor and capacitor in parallel.

When the components are connected in parallel, the impedances are not directly additive Instead the complex admittances, $Y^* = 1 / Z^*$, are directly additive. Thus total impedance,

$$Z^* = \frac{R(1/j\omega C)}{R + (1/j\omega C)} \tag{1.50}$$

$$= \frac{R}{1+\omega^2 C^2 R^2} + j\left(\frac{-\omega C R^2}{1+\omega^2 C^2 R^2}\right) \tag{1 51}$$

From the above equation the real part is,

$$Z' = \frac{R}{1+\omega^2 C^2 R^2} \tag{1 52}$$

and the imaginary part is,

$$Z'' = \frac{\omega C R^2}{1+\omega^2 C^2 R^2} \tag{1.53}$$

Eliminating ω from the above two equations, we get

$$Z'^2 + Z''^2 = RZ' \qquad (1\ 54)$$

or
$$\left(\frac{Z'-R}{2}\right)^2 + Z''^2 = \left(\frac{R}{2}\right)^2 \qquad (1\ 55)$$

This defines a semicircle in the complex impedance plane with a diameter, R, extending along the real axis from the origin This situation is represented in **Figure 1.7(b)**

These figures are obtained only when non-blocking electrodes, i e , the case wherein the mobile species participate in the electrode reactions. When blocking electrodes, i.e., electrodes different from the constituents of the electrolyte, are used, additional interface capacitance due to polarization comes into play In such cases, apart from the semicircle, a straight line especially at lower frequencies is also obtained in the complex impedance plane **Figure 1.8** shows such a situation wherein blocking electrodes are used

In real cases of polymer electrolytes, multiple polarization (with a capacitance CMP) is much effective due to surface layer formation at the electrodes, dielectric relaxation and ion-trapping, inhomogeneities in the polymer electrolyte and ion-ion interactions[62] So in the complex impedance plots one gets semicircles that are significantly broadened and depressed, i.e., the centre lies at a point lower than the real axis (as in **Figure 1.9**) However in those cases also the diameter is taken as a measure of the d c resistance of the electrolyte

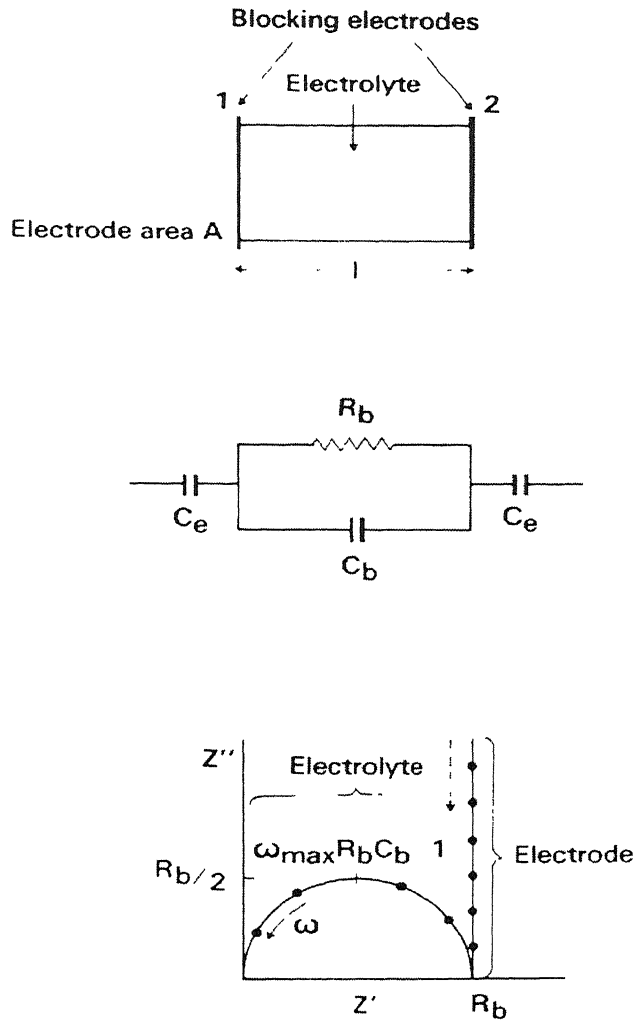

Figure 1.8 Schematic representation of a polymer electrolyte/blocking electrode cell. R_b = electrolyte resistance, C_b = electrolyte capacitance, C_e = electrode capacitance (ref. 62)

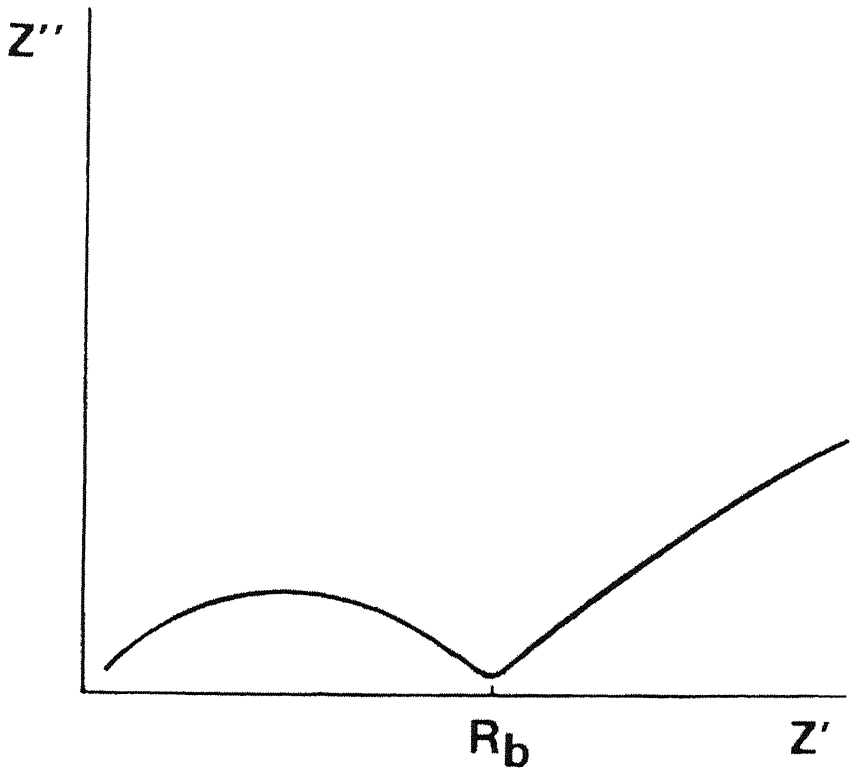

Figure 1.9 A typical complex impedance plot of a real polymer electrolyte/blocking electrode cell (ref. 62).

1.8 Statement of the problem

There is a growing demand for ionic conductors with more rigid specifications like higher conductivity at ambient temperatures, negligible change in conductivity with respect to temperature, low volume expansivity, etc.,. Several advantages of polymer electrolytes such as easy processability, mechanical flexibility, high conductivity, film formability, etc , make them a potential source for applications where ionic conductors are used Although PEO-metal salt complexes have reasonably high conductivities, their applications are limited to the fact that they have strong temperature dependent conductivities. This even applies to other polymer electrolytes such as polyphosphazene and polymethacrylate based comb like polymer electrolytes Inoue *et al*, reported the preparation of polymer electrolytes based on polystyrene derivatives with a pendant oligo(oxyethylene)cyclotriphosphazene side chain type comb-like polymers[63] They envisaged that if the oxyethylene chains form a continuous conducting phase around the rigid backbone, carrier ions could move in the phase, irrespective of the rigidity of the backbone, and a high conductivity would be expected.

The aim of this work is to prepare polymer electrolytes composed of polystyrene carrying pendant oligo(oxyethylene)cyclotriphosphazenes and sodium iodide and characterize them using the various techniques available. It is expected that the complex will be having linear and lesser temperature dependent conductivity It is also aimed to prepare a new polymer based on polystyrene carrying pendant branched oligo(oxyethylene)cyclotriphosphazene, which could serve as a better polymer host in electrolytic applications.

Synthesis and Characterization of poly(2-[(4′-vinyl-4-biphenylyl)oxy]-2,4,4,6,6-pentakis[2-(2-methoxy ethoxy)ethoxy]cyclotriphosphazene) and poly(2-[(4′-vinyl-4-biphenylyl)oxy]-2,4,4,6,6-pentakis[2,3-bis(2-(2-methoxy ethoxy)ethoxy)propoxy]cyclotriphosphazene)

The title polymers have been prepared using free radical polymerization technique The most commonly used methods for polymerization using free radicals are bulk polymerization and solution polymerization. In the bulk polymerization method, the monomer is polymerized by a free radical in the absence of a solvent while solution polymerization is carried out in a solvent The advantage of the latter technique is that the solvent helps in heat and mass transfer in the polymerization media The commonly used free radical initiators are azobisisobutyronitrile (AIBN), percarboxylic acids and their esters, hydrogen peroxide, etc , Since atmosphere contains oxygen that has an affinity towards free radicals, it is a must that the free radical polymerization reactions should be carried out in inert atmosphere conditions.

2.1 Measurements

The precursors, monomers and the polymers prepared were characterized using ^{1}H NMR, ^{31}P NMR, correlation spectroscopy (COSY) NMR, FT-IR and fast atom bombardment (FAB) and GC-MS mass spectroscopic techniques The various NMR spectra were recorded using a JEOL 400MHz NMR spectrophotometer. All the NMR spectra were recorded in $CDCl_3$ solvent using tetramethyl silane (TMS) as internal reference and the chemical shifts are reported in ppm FT-IR spectra were recorded as film in CH_2Cl_2 on Perkin-Elmer FT IR 1600 series model spectrophotometer FAB-Mass was recorded using JEOL SX 102/DA-6000 mass spectrophotometer using Xenon as the FAB gas GC-MS mass spectrum was recorded using Finnigan MD Family GC/MS Data system

2.2 Materials used

Hexachlorocyclotriphosphazene (Aldrich, USA) was recrystallized from hexane prior to use. 4-Hydroxybiphenyl (Loba Chemie, India), anhydrous aluminium chloride, anhydrous zinc chloride, sodium borohydride, formic acid, sodium hydroxide, hydrochloric acid, anhydrous magnesium sulphate, anhydrous potassium carbonate (S D Fine chemicals, India), trichloro acetic acid (Nice chemicals, India), 2-(2-methoxy ethoxy) ethanol, *p*-toluenesulphonyl chloride (Lancaster, UK), *t*-butyl glycidyl ether (Aldrich, USA), tetrafluoroboric acid(54% solution in diethyl ether) (Fluka, Switzerland) were used without any further purification The organic solvents were distilled and dried with appropriate drying agents according to standard literature procedures[65]. The initiator azoisobutyronitrile (AIBN) was recrystallized from methanol and vacuum dried before use Sodium hydride (Spetrochem, India) was purified with dry hexane

2.3 Synthesis of 2-(4′-vinyl-4-biphenylyloxy)pentachlorocyclotriphosphazene (CPHVB)

The synthesis of CPHVB was carried out as reported previously[66] The preparative details of the various components involved en route to CPHVB are given below

2.3.1 Preparation of 4-acetoxy-4′-acetyl biphenyl (AAB)

4-hydroxy biphenyl (80.0g, 0 47 mol) was added as solid in portions (~5 0g each) to an ice-cold solution of acetyl chloride (110.0g, 1.40 mol) and anhydrous $AlCl_3$ (160 0g, 1 20 mol) in 500 mL of dichloromethane with stirring over a period of thirty minutes The reaction mixture was stirred further for three hours at room temperature and poured into ice water. The methylene chloride solution was separated, washed with water and dried over anhydrous sodium sulphate. The solvent was removed by rotary evaporation to give a solid residue that was recrystallized from methanol to give AAB (110.0g, 96.7% yield, m.p. 124°C)

^{1}H NMR ($CDCl_3$) . δ 2 25 (3H, s, -OCOC$\underline{H}_3$); 2.55 (3H, s, -COC$\underline{H}_3$);

6.9 – 7.8 (8H, m, aromatic).

2.3.2 Preparation of 4-hydroxy-4′-hydroxyethyl biphenyl (HEB)

To a stirred solution of AAB (20.0g, 0.08 mol) in methanol (300 mL), a solution of sodium borohydride (3.0g, 0.08 mol) in methanol (100 mL) was added dropwise over a period of 30 minutes The resulting mixture was stirred at room temperature for 2 hours Most of the methanol was removed from the reaction mixture to yield an oil, to which 300 mL of ethyl acetate was added The ethyl acetate solution was washed with dilute HCl (3 x 300 mL) and water (3 x 300 mL) and dried over anhydrous sodium sulphate The ethyl acetate was then removed by rotary evaporation to obtain a solid residue, which was recrystallized from ethyl acetate to give pure HEB (16.0g, 98% yield, m.p 145°C)

^{1}H NMR ($CDCl_3$): δ 1 5 (3H, d, -C<u>H</u>$_3$); 4.9 (1H, q, -C<u>H</u><),

6.8 – 7.6 (8H, m, aromatic).

2.3.3 Preparation of 4-hydroxy-4′-vinyl biphenyl (HVB)

A mixture of HEB (20 0g, 0 09 mol) and anhydrous zinc chloride (4 0g, 0 09 mol) in 150 mL of DMSO was heated to 180 °C for 20 minutes in a 3 necked round-bottomed flask To this mixture, trichloro acetic acid (4.0g, 0.09 mol) was added in portions of 2 0g each and kept at the same temperature for an additional 3 hours along with stirring The resulting reaction mixture was allowed to cool to room temperature and poured into 2 litres of water. The resulting precipitate was filtered, washed repeatedly with water and was dried at room temperature It was then dissolved in 200 mL of acetone and extracted with hexane The combined hexane extracts were evaporated to give a semi-crystalline solid Recrystallization of this solid from benzene at room temperature afforded pure HVB (12 0g, 60% yield, m.p. 192°C).

^{1}H NMR ($CDCl_3$) : δ 5 1 – 6 6 (3H, -C<u>H</u>=C<u>H</u>$_2$); 6.8 – 7 5 (8H, aromatic)

2.3.4 Preparation of 2-(4'-vinyl-4-biphenylyloxy)pentachlorocyclotriphosphazene (CPHVB)

To a stirred solution of hexachlorocyclotriphosphazene ($N_3P_3Cl_6$, 10 6g, 0 03 mol) in 100 mL of dry benzene, a solution of HVB (6.0g, 0 04mol) and triethylamine (4 0 mL, 0 04 mol) in 100 ml of dry benzene was added dropwise for 30 minutes at room temperature The resulting mixture was stirred for an additional 4 hours at room

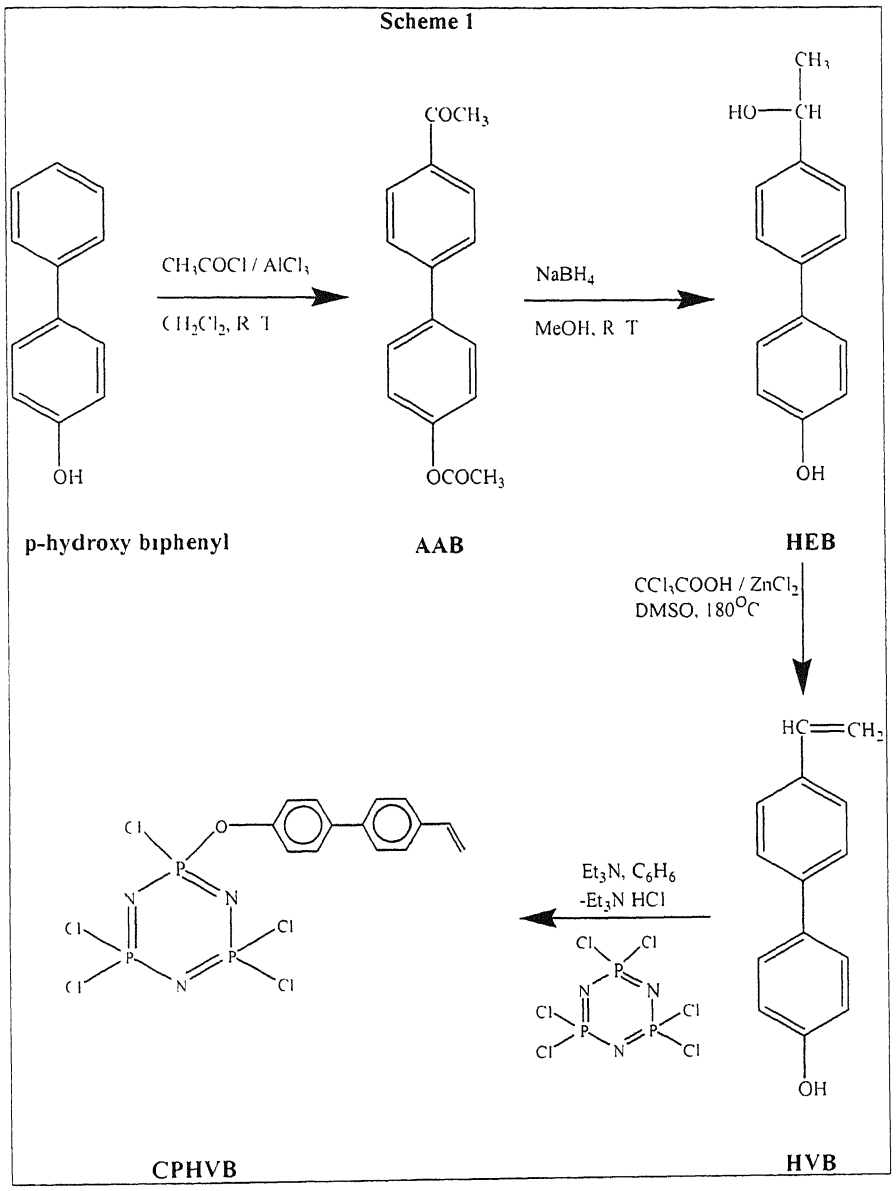

temperature The amine hydrochloride formed in the reaction was removed by filtration. The solvent benzene was stripped off from the filtrate under reduced pressure to give a colourless oil. CPHVB was separated from the unreacted $N_3P_3Cl_6$ by subjecting the oil to column chromatography (silica gel, 60 – 120 mesh) using hexane as the eluent The CPHVB thus obtained was recrystallized from hexane to get pure CPHVB (40% yield, m p 112°C)

^{1}H NMR ($CDCl_3$)· δ 5.28(dd, =C$\underline{H}_2$); 5.75(dd, =C$\underline{H}_2$); 6.78(dd, -C$\underline{H}$=); 7 2 – 7 68(m, aromatic)

^{31}P NMR ($CDCl_3$) δ 20.8 (d, P(Cl)(OR)); 10.6 (t, PCl_2).

The preparation of CPHVB is outlined in **Scheme 1**.

2.4 Synthesis of poly(2-[(4′-vinyl-4-biphenylyl)oxy]-2,4,4,6,6-pentakis[(2-methoxy ethoxy]cyclotriphosphazene) (PPMEE)

The polymer, PPMEE, was prepared by a method reported by Inoue *et.al.*,[63].

2.4.1 Synthesis of 2-[(4′-vinyl-4-biphenylyl)oxy]-2,4,4,6,6-pentakis[(2-methoxy ethoxy)ethoxy]cyclotriphosphazene (PMEE)

2.4.1.1 Preparation of the sodium salt of 2-(2-methoxy ethoxy)ethanol

To a suspension of NaH (0 57g, 0.023mol) in dry THF (50 mL), a solution of 2-(2-methoxy ethoxy)ethanol (2.85g, 0.023mol) in 100mL of dry THF was added dropwise for a period of thirty minutes. The resulting mixture was stirred until no hydrogen evolved from the reaction flask

2.4.1.2 Preparation of PMEE

To the solution of the sodium salt of 2-(2-methoxy ethoxy)ethanol in dry THF prepared as above, CPHVB (2.0g, 3.94 mmol) in 100mL of dry THF was added dropwise with continuous stirring After the addition was over the reaction mixture was heated under reflux for 24 hours in dry nitrogen atmosphere. The reaction mixture was then cooled to room temperature and the NaCl formed filtered off using a sintered funnel The filtrate was subjected to rotary evaporation to yield a brown oil. This oil was subjected to column chromatography (silica gel, 100 – 200 mesh) with a mixture of hexane and

ethylacetate as the eluent Using thin-layer chromatography, fractions containing pure PMEE were identified and were evaporated under reduced pressure to yield pure PMEE

^{1}H NMR ($CDCl_3$) δ 3.31 – 4.21(m, 55H, -OCH_2CH_2-OCH_2CH_2-OCH_3)
5.27 (d, 1H, =CH_2); 5.78 (d, 1H, =CH_2), 6.75 (dd, 1H, -CH=),
6.97 – 7.53(m, 8H, aromatic).

^{31}P NMR ($CDCl_3$). δ 14.4 (t, P(OR)(Obiphen)); 17.6 (d, P(OR)(OR))

FAB-Mass: (m/z) 926 (M^+)

2.4.2 Polymerization of PMEE

A solution of the monomer (5.0g, 0.75mol/L) in 7.2mL of dichloroethane and AIBN (0.0453g, 2.4mmol/L) was bubbled with argon gas for thirty minutes and then heated at 70° to 80 °C for 24 hours in dry argon atmosphere under constant stirring. The reaction flask was then cooled and the solution was poured into large quantities of hexane The polymer was thrown out in this process. The polymer thus obtained was dissolved in a minimum amount of THF and again poured into large quantities of hexane This procedure was repeated several times until the hexane solution was colorless The pure polymer was obtained by completely removing the solvent under reduced pressure The polymer obtained was a highly viscous light yellow coloured liquid.

^{1}H NMR ($CDCl_3$)· δ 3.24 – 4.16 (m, -OCH_2-), 7.24 – 7.48 (m, aromatic)

^{31}P NMR ($CDCl_3$)· δ 14.3 (t, P(OR)(Obiphen)); 17.6 (d, P(OR)(OR))

IR(neat) cm^{-1}: 2880(vs); 1493(m); 1232(vs); 1198(w); 1047(s)

2.5 Synthesis of poly(2-[(4′-vinyl-biphenylyl)oxy]-2,4,4,6,6-pentakis[2,3-bis(2-(2-methoxy ethoxy)ethoxy)propoxy)cyclotriphosphazene) (PPOMEE)

The procedure for the preparation of PPOMEE is given below.

2.5.1 Synthesis of 2-[(4′-vinyl-biphenylyl)oxy]-2,4,4,6,6-pentakis[2,3-bis(2-(2-methoxy ethoxy)ethoxy)propoxy]cyclotriphosphazene (POMEE)

2.5.1.1 Preparation of 2,3-bis(2-(2-methoxy ethoxy)ethoxy)propanol (HOMEE)

HOMEE was prepared following the procedure reported by Allcock *et al*.,[67]

ethylacetate as the eluent. Using thin-layer chromatography, fractions containing pure PMEE were identified and were evaporated under reduced pressure to yield pure PMEE

^{1}H NMR ($CDCl_3$) δ 3.31 – 4.21(m, 55H, -OC$\underline{H}_2$C$\underline{H}$,-OC$\underline{H}_2$C$\underline{H}_2$-OC$\underline{H}_3$)
5.27 (d, 1H, =C$\underline{H}_2$); 5.78 (d, 1H, =C$\underline{H}_2$); 6.75 (dd, 1H, -C$\underline{H}$=),
6.97 – 7.53(m, 8H, aromatic)

^{31}P NMR ($CDCl_3$) δ 14.4 (t, P(OR)(Obiphen)), 17.6 (d, P(OR)(OR))

FAB-Mass (m/z) 926 (M^+)

2.4.2 Polymerization of PMEE

A solution of the monomer (5.0g, 0.75mol/L) in 7.2mL of dichloroethane and AIBN (0.0453g, 2.4mmol/L) was bubbled with argon gas for thirty minutes and then heated at 70° to 80 °C for 24 hours in dry argon atmosphere under constant stirring. The reaction flask was then cooled and the solution was poured into large quantities of hexane. The polymer was thrown out in this process. The polymer thus obtained was dissolved in a minimum amount of THF and again poured into large quantities of hexane. This procedure was repeated several times until the hexane solution was colorless. The pure polymer was obtained by completely removing the solvent under reduced pressure. The polymer obtained was a highly viscous light yellow coloured liquid.

^{1}H NMR ($CDCl_3$): δ 3.24 – 4.16 (m, -OC$\underline{H}_2$-), 7.24 – 7.48 (m, aromatic)

^{31}P NMR ($CDCl_3$): δ 14.3 (t, P(OR)(Obiphen)); 17.6 (d, P(OR)(OR))

IR(neat) cm^{-1}: 2880(vs); 1493(m); 1232(vs); 1198(w); 1047(s)

2.5 Synthesis of poly(2-[(4′-vinyl-biphenylyl)oxy]-2,4,4,6,6-pentakis[2,3-bis(2-(2-methoxy ethoxy)ethoxy)propoxy)cyclotriphosphazene) (PPOMEE)

The procedure for the preparation of PPOMEE is given below

2.5.1 Synthesis of 2-[(4′-vinyl-biphenylyl)oxy]-2,4,4,6,6-pentakis[2,3-bis(2-(2-methoxy ethoxy)ethoxy)propoxy]cyclotriphosphazene (POMEE)

2.5.1.1 Preparation of 2,3-bis(2-(2-methoxy ethoxy)ethoxy)propanol (HOMEE)

HOMEE was prepared following the procedure reported by Allcock. *et al*.[67]

2.5.1.2 Preparation of 3-*tert*-butoxy-1,2-propanediol (TBOH)

t-Butyl glycidyl ether (5.52g, 0.0424mol) was added dropwise to 99% formic acid (3.9g, 0.0848mol). During the addition, the reaction mixture was stirred and the temperature maintained below 30 °C. The mixture was stirred further for a period of 12 hours at room temperature. A solution of sodium hydroxide (4.24g, 0.106mol) in 4.3 mL of water was added slowly with the temperature maintained below 40 °C. The organic fraction was separated and the aqueous phase was extracted several times with dichloromethane. The combined organic fractions were dried with anhydrous $MgSO_4$ and evaporated to get an oily residue, which was distilled under vacuum to give pure TBOH as a colourless oil (54% yield, b.p. 55 – 60 °C/0.015 torr).

^{1}H NMR ($CDCl_3$): δ 2.91 - 3.61 (m, 7H); 1.21 (s, 9H, $\underline{Me}_3$-C-)

IR(neat) cm^{-1}: 3391(s); 2974(vs); 2932(s), 1472(w); 1365(m); 1196(s), 1083(vs), 883(w)

2.5.1.3 Preparation of 2-(2-methoxy ethoxy)ethyl *p*-toluenesulphonate (MEETS)

A slurry of *p*-toluenesulphonyl chloride (13.4g, 0.0703mol) and pyridine (14.2 mL) was stirred in a three-necked argon-filled flask. The temperature of the reaction mixture was maintained below 5 °C. To this, 2-(2-methoxy ethoxy)ethanol (8.44g, 0.0703mol) was added slowly from an addition funnel. After the addition was complete, the mixture was stirred for 15 minutes and then poured into ice-cold water (90mL) and washed with dichloromethane (90 mL). The organic layer was separated, washed with ice-cold 6N HCl (3 x 160 mL), dried with anhydrous $MgSO_4$ and reduced to a minimum volume by evaporation to yield MEETS as a colorless oil (61% yield).

^{1}H NMR ($CDCl_3$): δ 2.45 (s, 3H, -OC$\underline{H}_3$); 3.35 (s, 3H, Ar-C$\underline{H}_3$), 3.47 – 4.18 (m, 8H); 7.34 (d, 2H, aromatic); 7.8 (d, 2H, aromatic)

2.5.1.4 Preparation of 1-(*tert*-butyloxy)-2,3-bis(2-(2-methoxy ethoxy)ethoxy propane (TBMEE)

The sodium salt of TBOH was prepared first as follows. To a solution of NaH (5.66g, 0.236mol) in dry THF (50 mL), a solution of TBOH (7.0g, 0.0472mol) in 100mL of dry THF was added dropwise for a period of thirty minutes and the resulting mixture was stirred until no hydrogen evolved from the reaction flask. This mixture was refluxed

and a solution of MEETS (25 9g, 0.0994mol) in 300 mL of dry THF was added dropwise under refluxing conditions The reaction mixture was stirred, heated under reflux under

Scheme 2

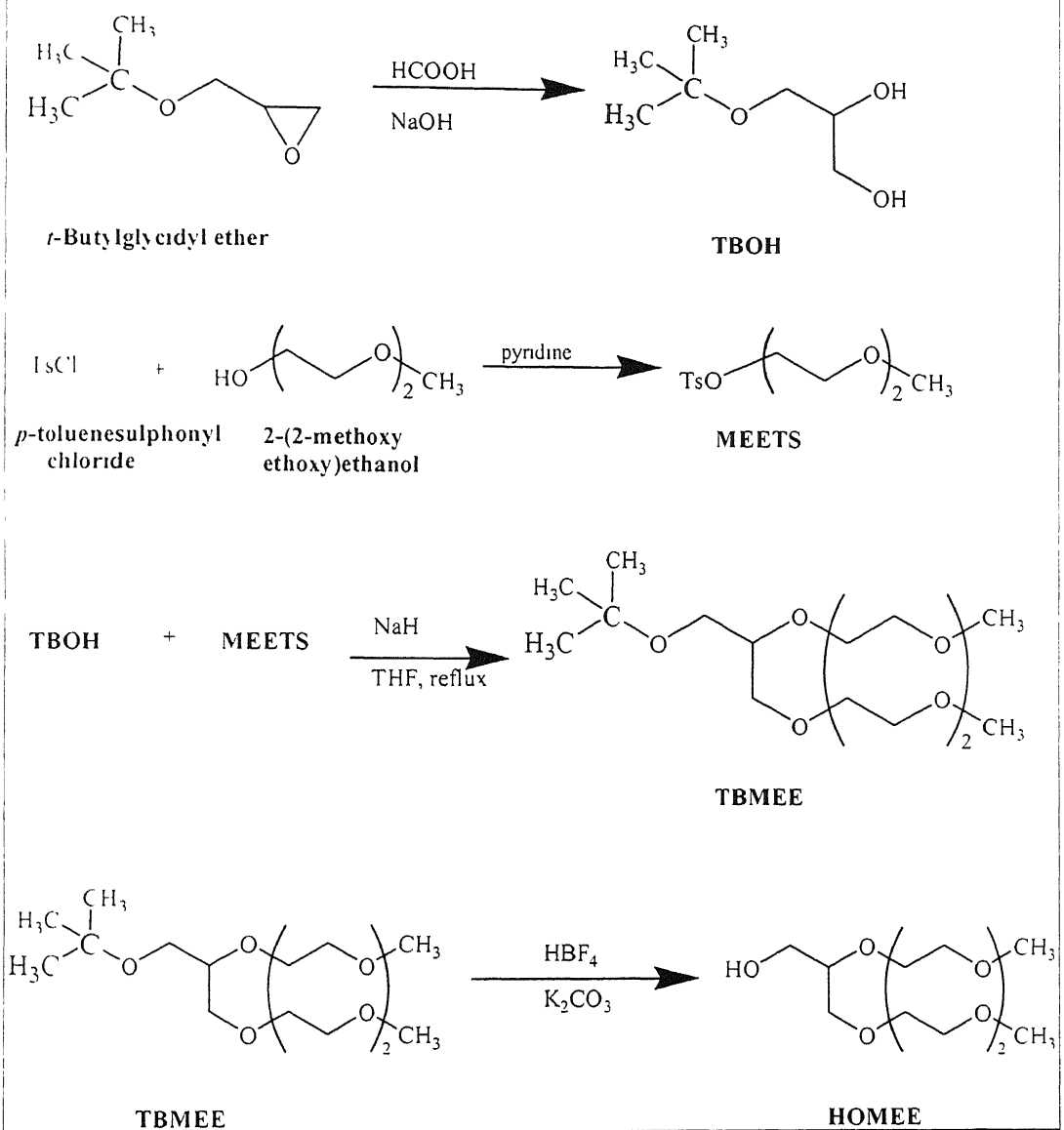

an atmosphere of dry N_2 for 24 hours. The mixture was allowed to cool, filtered and the solvent was removed by evaporation under vacuum. The residue was dissolved in chloroform, washed with water, dried ($MgSO_4$) and the solvent removed in vacuo to yield a brown liquid. This was subjected to column chromatography (silica gel, 100 – 200 mesh) with hexane-ethylacetate mixtures as the eluent and pure TBMEE was obtained as a colorless liquid (35% yield) after evaporation of the solvent

^{1}H NMR ($CDCl_3$) δ 1 21 (s, 9H), 2 91 – 3.61 (m, 27H)

2.5.1.5 Preparation of HOMEE

To a solution of TBMEE (13.38g, 0 038mol) in dichloromethane (50mL), tetrafluoroboric acid (8 02mL) was added dropwise. The mixture was stirred at room temperature for 20 minutes. The acid was neutralized with excess solid potassium carbonate, the inorganic salts filtered off and the solvent was removed by rotary evaporation to give a pale yellow oil. The crude product was distilled under vacuum (~140°C) to remove the remaining inorganic salts. The residue was subjected to column chromatography (silica gel, 100 – 200 mesh) with ethylacetate-THF mixtures as the eluent The product, HOMEE, was obtained in the pure form as a colourless liquid (49% yield), after evaporation of the solvent.

^{1}H NMR ($CDCl_3$): δ 3 21 – 3.79 (m, 27H)

Mass spectrum: 297 (M^+)

The synthesis of HOMEE is represented in **Scheme 2**

2.5.2 Preparation of POMEE

To a solution of the sodium salt of HOMEE (prepared by adding a solution of HOMEE (2 38g, 0.008mol) in dry THF to a stirred suspension of NaH (0.192g, 0 008mol) in THF and stirring the mixture continuously until reaction is complete), in dry THF, CPHVB (0.675g, 1 33mmol) in 100mL of dry THF was added dropwise with continuous stirring. After the addition was over the reaction mixture was refluxed for 24 hours in dry nitrogen atmosphere. The reaction mixture was then cooled to room temperature and the NaCl formed filtered off using a sintered funnel. The filtrate was subjected to rotary evaporation to yield a yellow coloured oil. This oil was subjected to column chromatography (neutral alumina) with ethylacetate-THF and THF-methanol mixtures as eluents. Fractions containing pure POMEE were identified using thin layer chromatography and were evaporated under reduced pressure to yield pure POMEE as a light yellow oil.

^{1}H NMR ($CDCl_3$): δ 3.25 – 3.86 (m, 135H); 5.2 (d, 1H, -CH_2-); 5.72 (d, 1H,CH_2); 6.67 (dd, 1H, -CH=); 6.82 – 7.47 (m, 8H, aromatic).

^{31}P NMR ($CDCl_3$). δ 14 2 (t, P(OR)(Obiphen)); 17.5 (d, P(OR)(OR))

FAB-Mass 1806 (M^+)

2.5.3 Polymerization of POMEE

A solution of POMEE (1 07g, 0.593mol/L) in 2 mL of dichloroethane and AIBN ($3\ 12\times10^{-3}$g, $1\ 9\times10^{-2}$mol/L) was bubbled with argon gas for thirty minutes and then heated at 70° to 80°C for 24 hours in dry argon atmosphere with continuous stirring The reaction flask was then cooled and the solution was poured in large quantities of hexane The polymer thrown out in this process was dissolved in a minimum amount of THF and again poured into large quantities of hexane This procedure was repeated several times until the hexane solution was colorless. The pure polymer, PPOMEE, was obtained by completely removing the solvent under reduced pressure The polymer obtained was a gel-like colourless material

^{1}H NMR ($CDCl_3$) δ 1 59 - 2.43 (m, 3H, -C<u>H</u>-C<u>H$_2$</u>-), 3.23 – 4 14 (m, broad, 135H), 6.95 – 7 77 (m, broad, 8H, aromatic)

^{31}P NMR ($CDCl_3$) δ 13.8 (t, broad, P(OR)(Obiphen); 17.5 (d, P(OR)(OR))

2.6 Results and discussion

2.6.1 Synthesis and Characterization of PPMEE

The polymer, PPMEE was synthesized as shown in **Scheme 3**. The reaction involving the substitution of P-Cl bonds in CPHVB was done in N_2 atmosphere and in dry conditions. The polymer, PPMEE is a stable highly viscous liquid, soluble in a variety of organic solvents such as THF, dichloromethane, methanol, ethanol, etc ,. The monomer was characterized using ^{1}H NMR, ^{31}P NMR and FAB-Mass spectroscopic techniques. The polymer was characterized using ^{1}H NMR, ^{31}P NMR and IR techniques The spectra of the monomer and the polymer are shown in **Figures 2.1** to **2.6** respectively The absence of the peaks at δ = 5.27 (d, 1H, =CH_2), 5.78 (d, 1H, =CH_2) and 6 75 (dd, 1H, -CH=) due to the vinyl group (present in the monomer, PMEE) in the ^{1}H NMR spectrum of PPMEE, confirms the formation of the polymer ^{31}P NMR spectrum of the monomer, PMEE shows the presence of oligoethyleneoxy side-chains on the cyclophosphazene ring as there is a shift in the peaks (δ 14.41 (t, P(OR)(Obiphen)), 17 61

(d, P(OR)(OR))) when compared to the ^{31}P NMR of CPHVB (δ 20.8 (d, P(Cl)(Obiphen)), 10 62 (t, PCl_2). FAB-Mass of the monomer shows a molecular ion peak at 926 The IR spectrum of PPMEE shows the -CH_2- stretching of the polymer backbone by the band at

Scheme 3

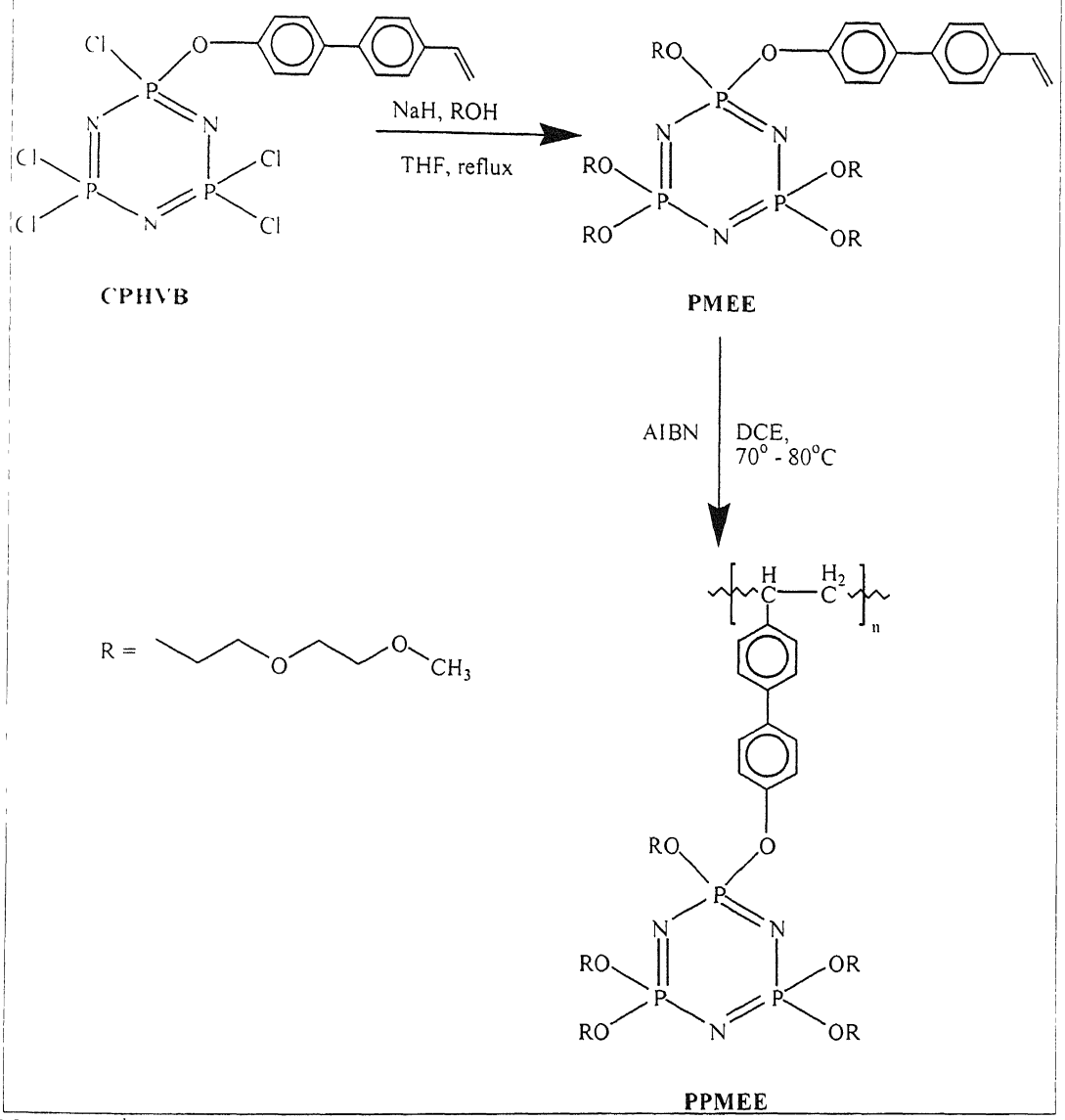

2837.7cm^{-1} The -C-O-C- stretching of the oligoethyleneoxy side-chains are observed at 1112cm^{-1} The P=N stretching gives a band at 1232.9 cm^{-1}.

2.6.2 Synthesis and Characterization of PPOMEE

The synthesis of PPOMEE is shown in **Scheme 4**. This polymer is expected to act as a very good host for metal salts due to the large number of basic sites present. The

Scheme 4

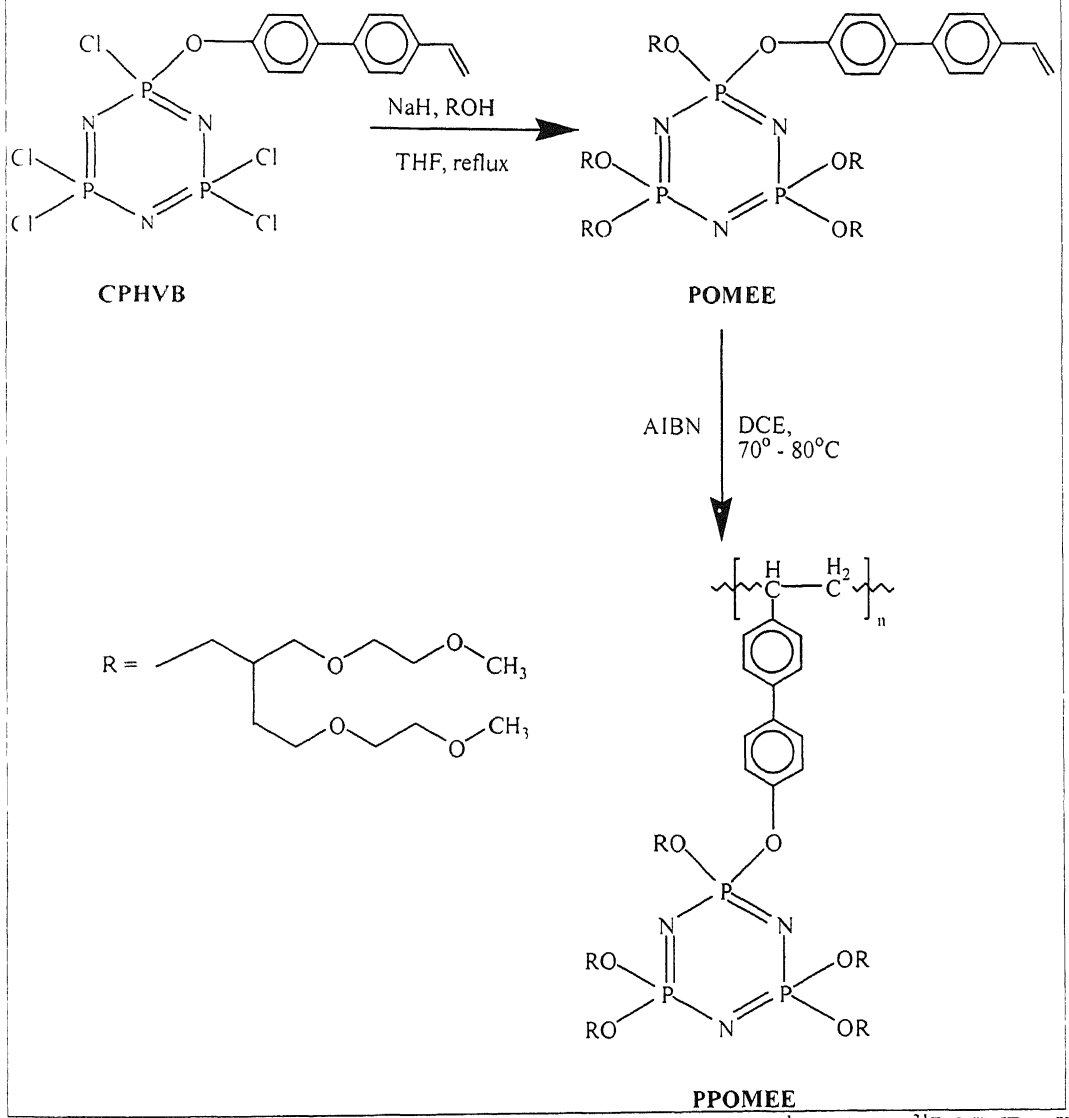

precursors, monomer and the polymer were characterized using ^{1}H NMR, ^{31}P NMR, IR, FAB-Mass and GC-MS methods. The diol precursor, TBOH was characterized using ^{1}H NMR and IR studies. ^{1}H NMR of the precursor shows a singlet corresponding to the Me_3C- group and a multiplet, which is due to and etheroxy groups. To confirm the cleavage of the epoxide ring to form the diol, IR spectrum, shown in **Figure 2.7**, was

recorded The broad -OH stretching band at 3391.4 cm^{-1} confirms this. The toluene sulphonate precursor, MEETS was characterized using ^1H NMR The spectrum shows two doublets due to aromatic protons in addition to the multiplets due to etheroxy protons and singlets due to Ar-CH_3 and –OCH_3 groups. The reaction between *p*-tosylchloride and 2-(2-methoxy ethoxy)ethanol is carried out under extremely dry conditions, since *p*-tosylchloride is highly hygroscopic and the presence of water inhibits the reaction. The reaction between MEETS and TBOH takes place with the elimination of sodium tosylsulphonate ^1H NMR of the product, TBMEE shows that the tosyl group has been completely removed (absence of the peaks due to aromatic protons). Employing a mild acid such as HBF_4 brings about cleavage of the tert-butyl group in the next step, since the use of strong acids like trifluoroacetic acid would result in the cleavage of other C-O bonds present in the compound In the ^1H NMR of HOMEE the singlet due to Me_3C-group is absent The GC-MS of HOMEE showed a molecular ion peak at 297 The reaction of the alcohol, HOMEE with CPHVB is carried out under dry N_2 atmosphere and dry reaction conditions The monomer, POMEE, formed by the substitution of P-Cl bonds in CPHVB was characterized using ^1H NMR, ^{31}P NMR and FAB-Mass. The shifts in the δ-values in the ^{31}P NMR of POMEE (δ 13.8 (t, broad, P(OR)(Obiphen)); 17.5 (d, P(OR)(OR)) as compared to that of CPHVB prove the substitution of chlorines by the branched oligoethyleneoxy side-chains in the cyclophosphazene rings The ^{31}P NMR of POMEE is given in **Figure 2.8** The proton NMR of POMEE, as in **Figure 2.9**, gave a very broad multiplet for the oligoethyleneoxy side-chains. Hence in a view to study this region further and assign the peaks specifically to the different types of -CH_2O- and -OCH_3 groups ^1H-^1H 2D COSY NMR of POMEE was recorded. The basic COSY procedure gives a 2D spectrum from which almost all the ^1H-^1H connectivities can be determined The ^1H NMR spectrum appears along the diagonal as contours representing peak intensities. The off-diagonal peaks are called 'cross-peaks'. A horizontal line drawn from a cross-peak will intercept a contour on the diagonal with which the first diagonal contour is correlated, that is coupled. The cross-peaks are found symmetrically on both sides of the diagonal. For convenience the derived ^1H spectrum may be projected along one or both the axes. A line drawn perpendicular to a peak in the projected spectrum will intersect in the diagonal spectrum and indicate the appropriate contour even in an

overlapping region The 2D ^{1}H-^{1}H NMR spectrum of POMEE is shown in **Figure 2.10** Here except for the connectivities of the vinyl and aromatic protons, the contours obtained for the oligoethyleneoxy protons were very much diffused Hence the assignment of the peaks corresponding to the different kinds of $-OCH_2CH_2O-$ and $-OCH_3$ groups was not possible ^{1}H NMR spectra at low temperatures (0, -20, -40 and –50 °C) were also recorded to establish the assignments. But the lower the temperature employed the peaks due to oligoethyleneoxy groups broadened more This may be due to the restriction in the orientational freedom of the side-chain segments, which reduces the interaction between the spinning nuclei. A comparison of the ^{1}H NMR spectra recorded at various temperatures is shown in **Figure 2.11**. Polymerization of POMEE was carried out in extremely dry conditions in the absence of oxygen. This process yielded a gel-like material, which was characterized using ^{1}H NMR and ^{31}P NMR The respective spectra are shown in **Figures 2.12** and **2.13** The absence of the resonances due to the vinyl group in the proton NMR spectrum confirms the formation of the polymer. The invariance of the ^{31}P NMR patterns in the monomer and the polymer proves the retention of the cyclophosphazene motif in the polymer.

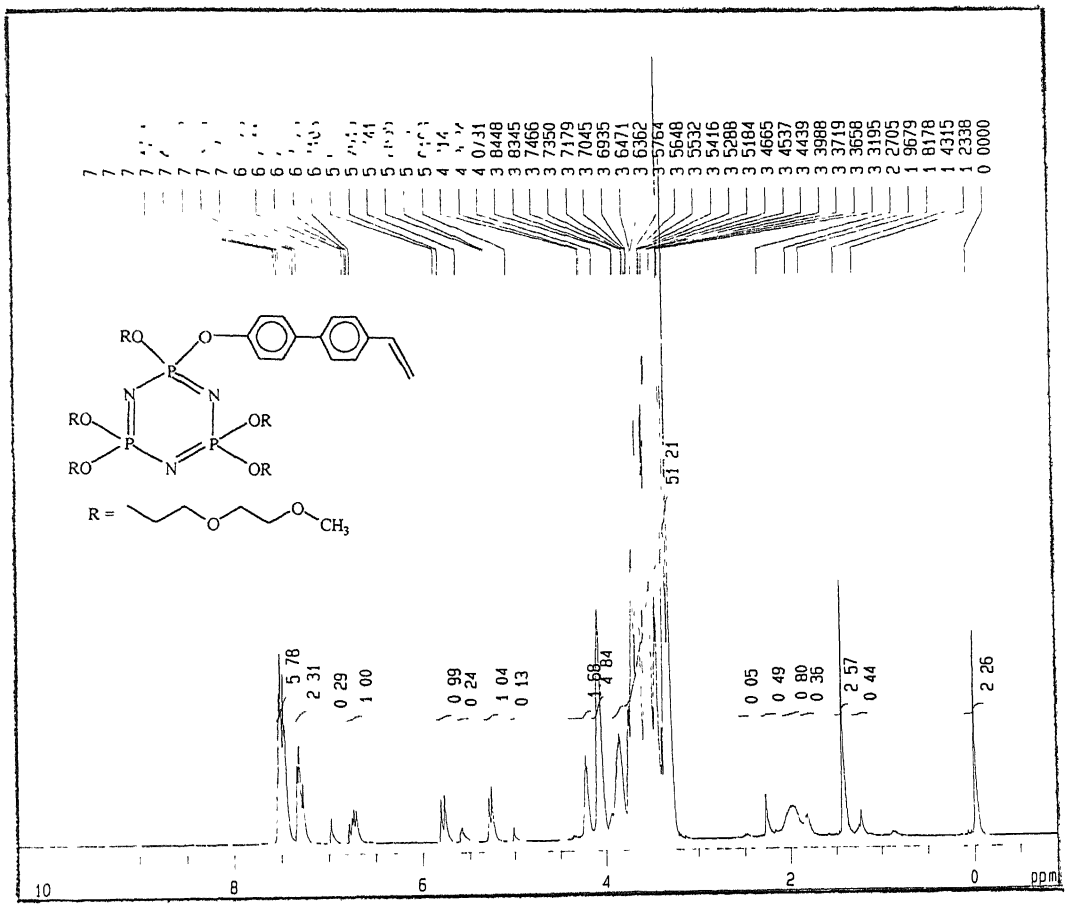

Figure 2.1 ^{1}H NMR spectrum of PMEE

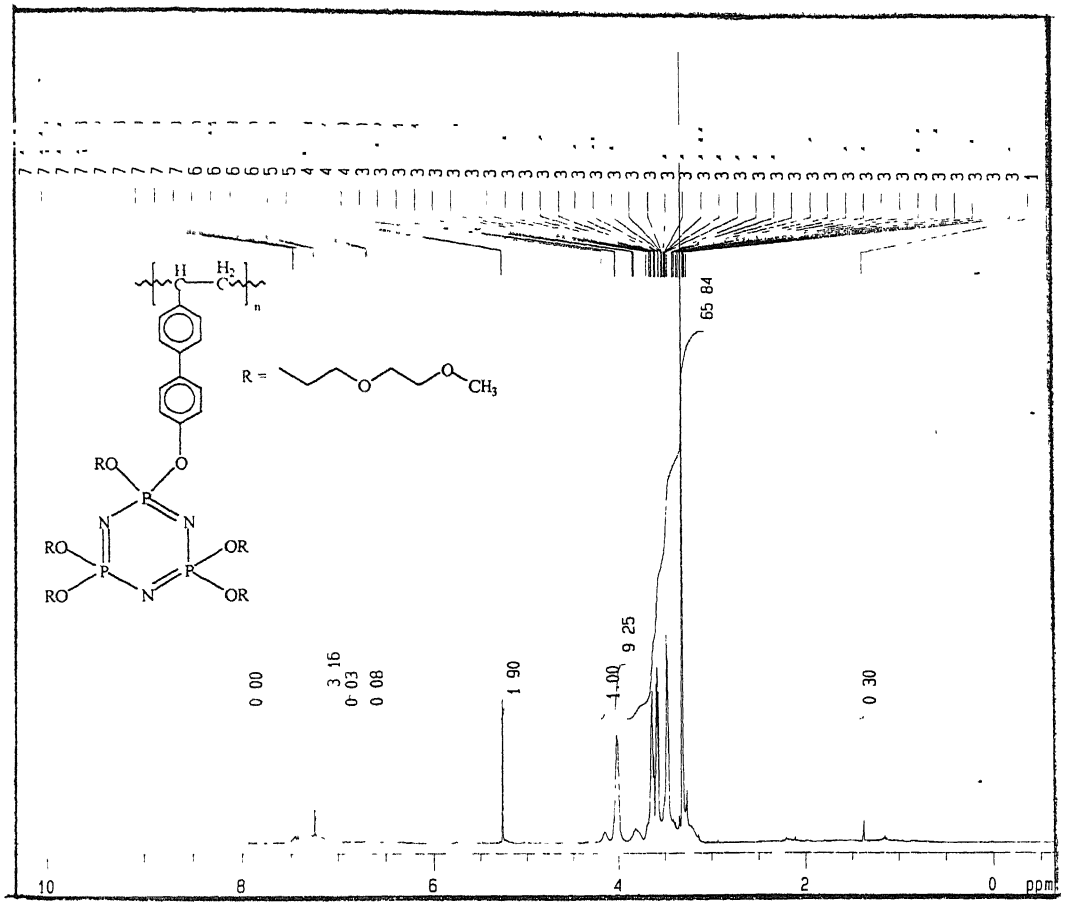

Figure 2.2 ^{1}H NMR spectrum of PPMEE

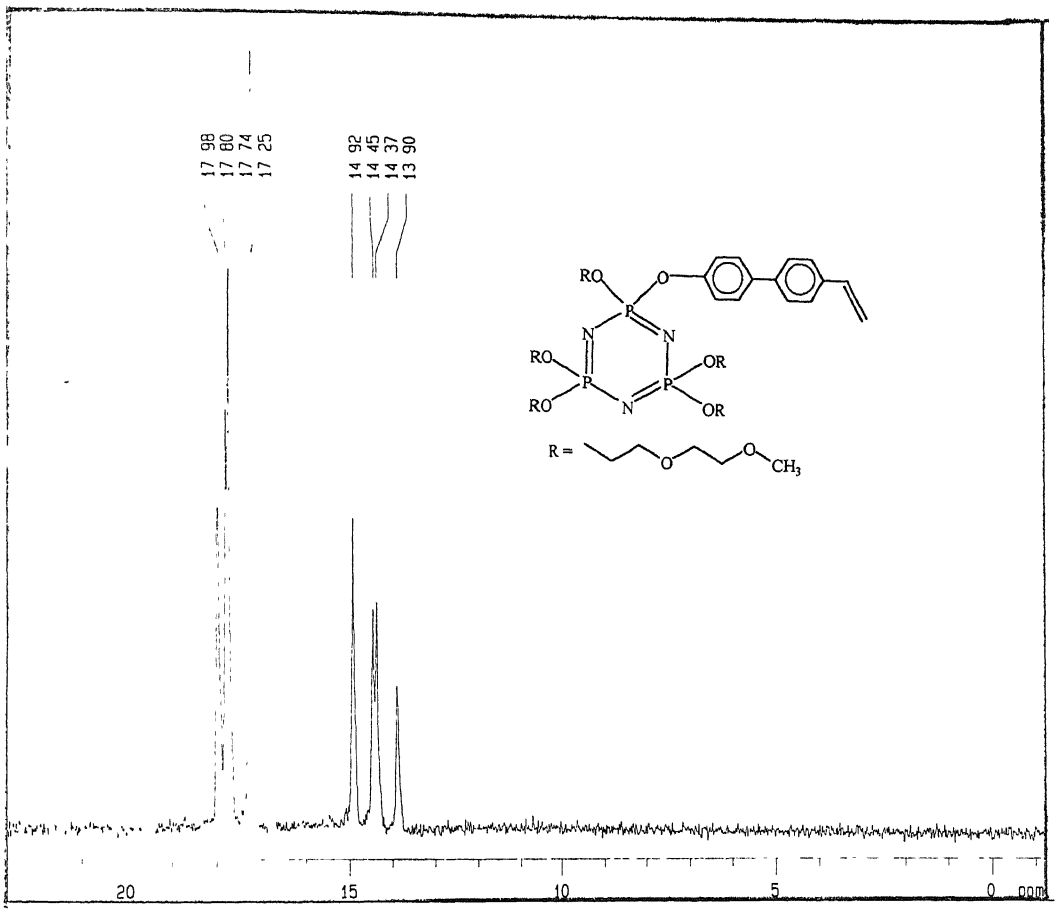

Figure 2.3 ^{31}P NMR spectrum of PMEE

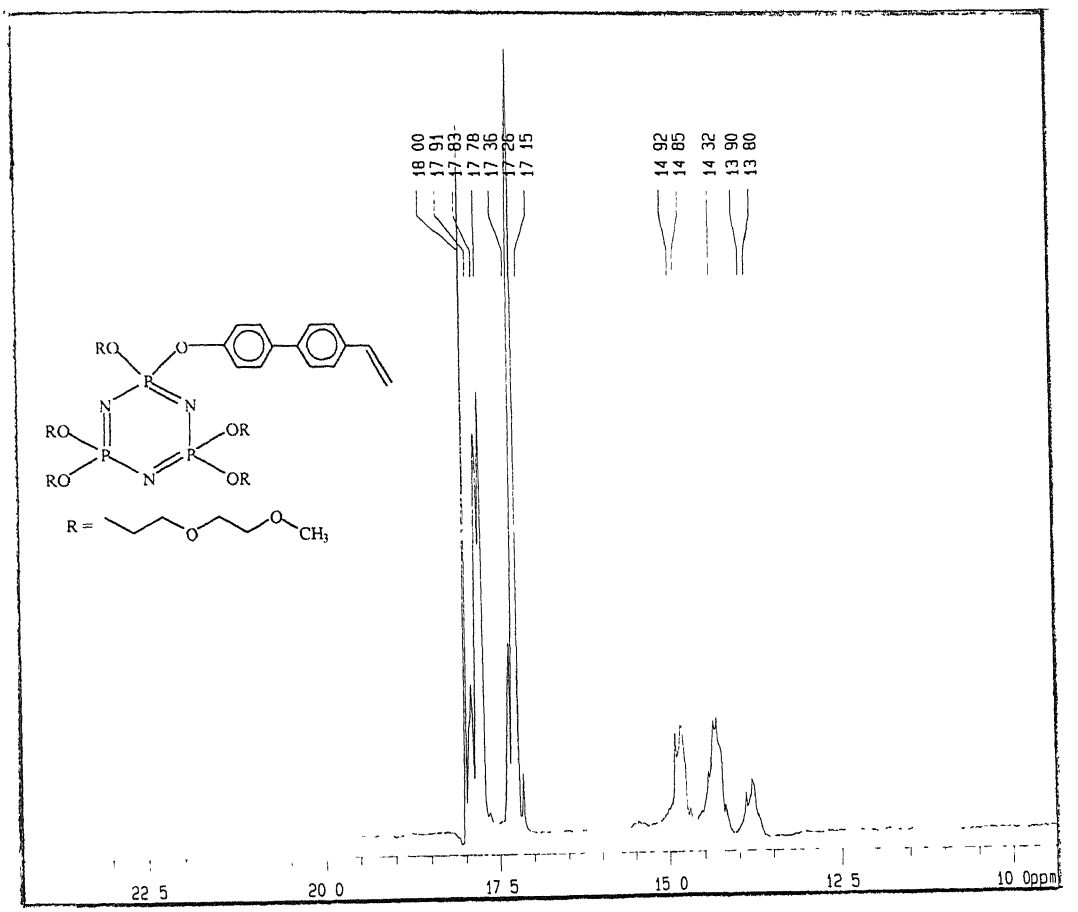

Figure 2.4 ^{31}P NMR spectrum of PPMEE

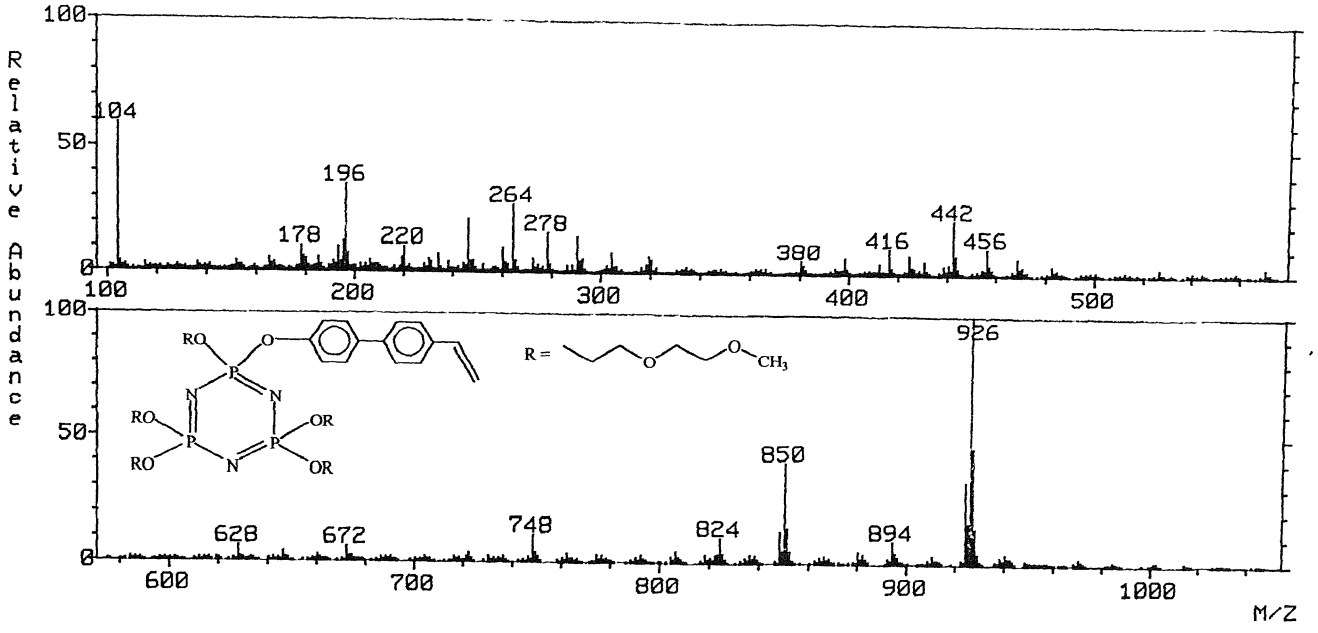

Figure 2.5 FAB-Mass spectrum of PMEE

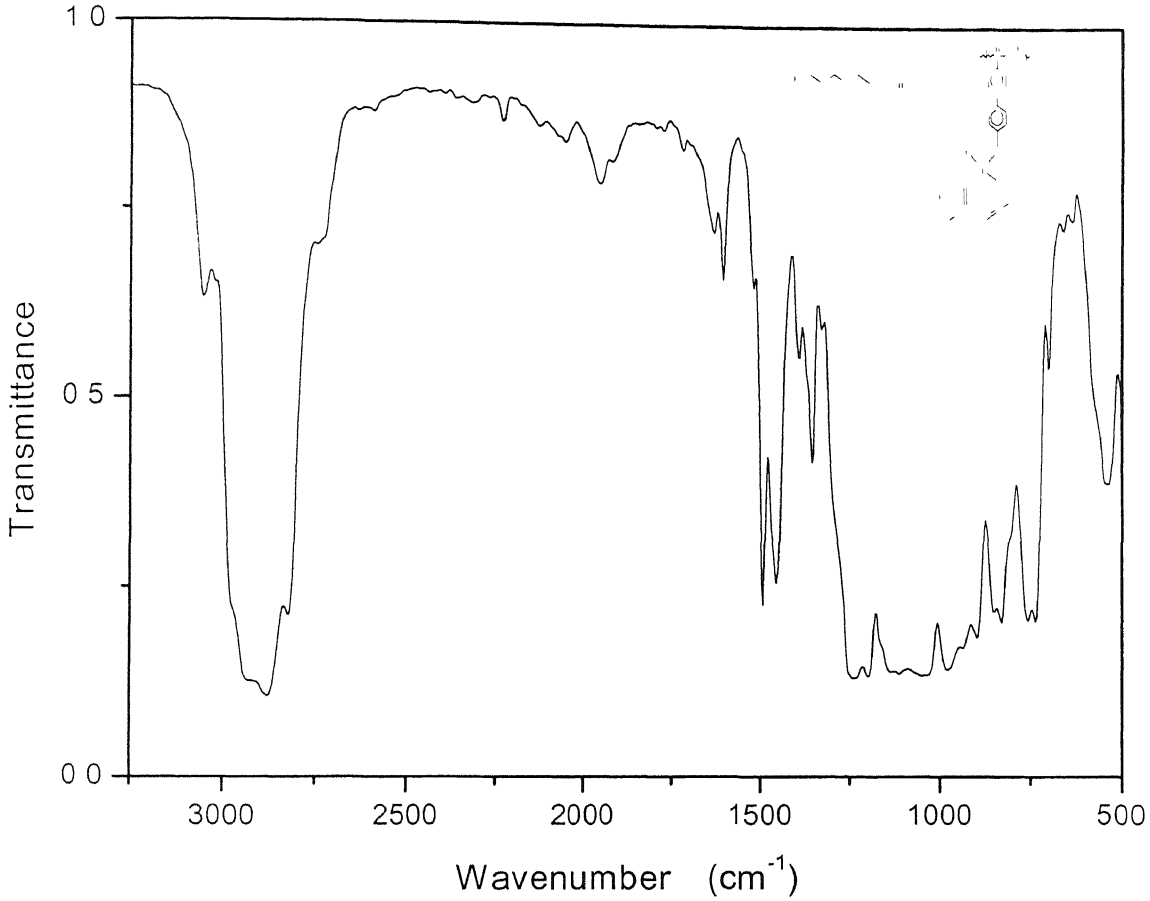

Figure 2.6 IR spectrum of PPMEE

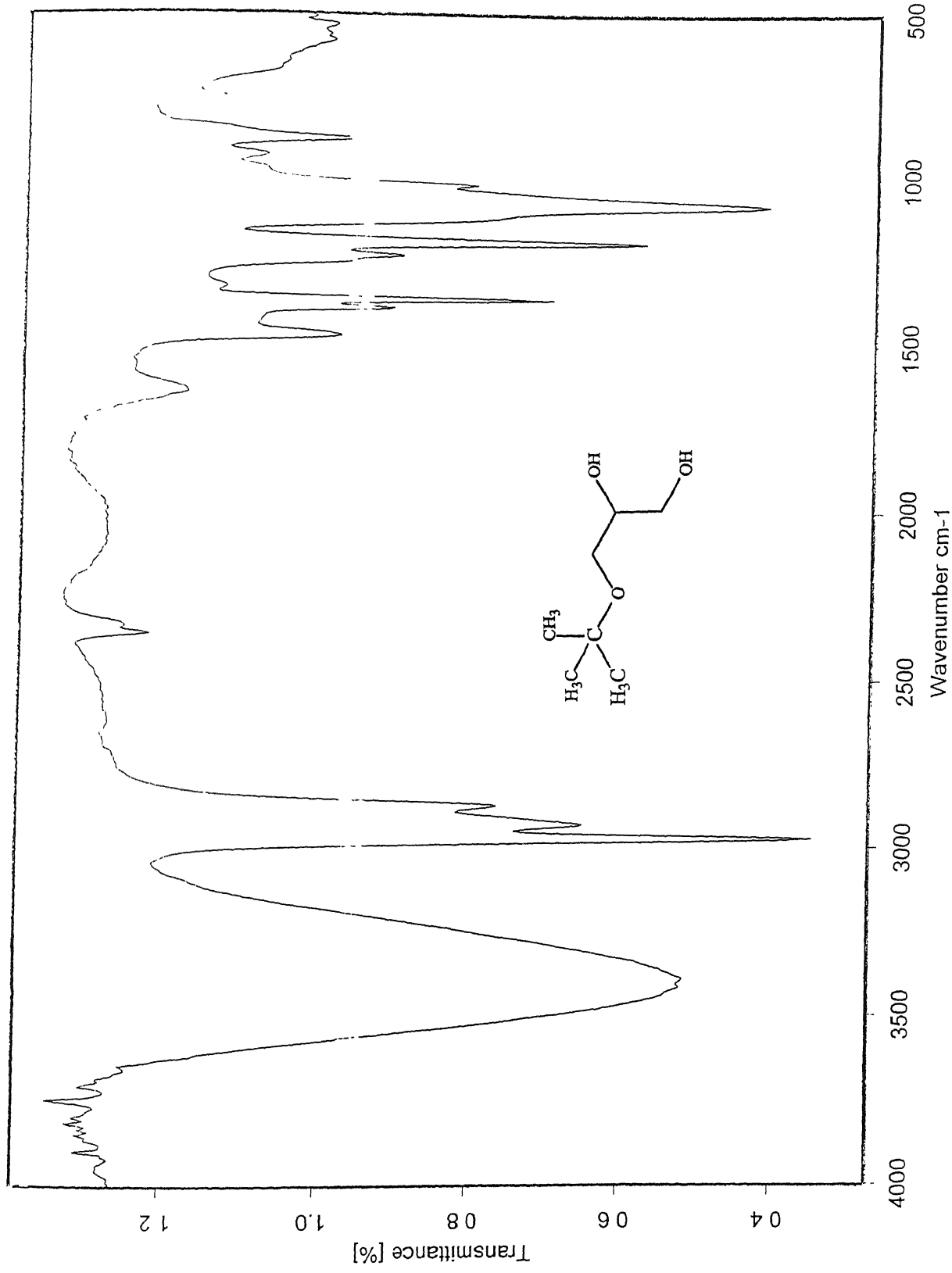

Figure 2.7. IR spectrum of TBOH

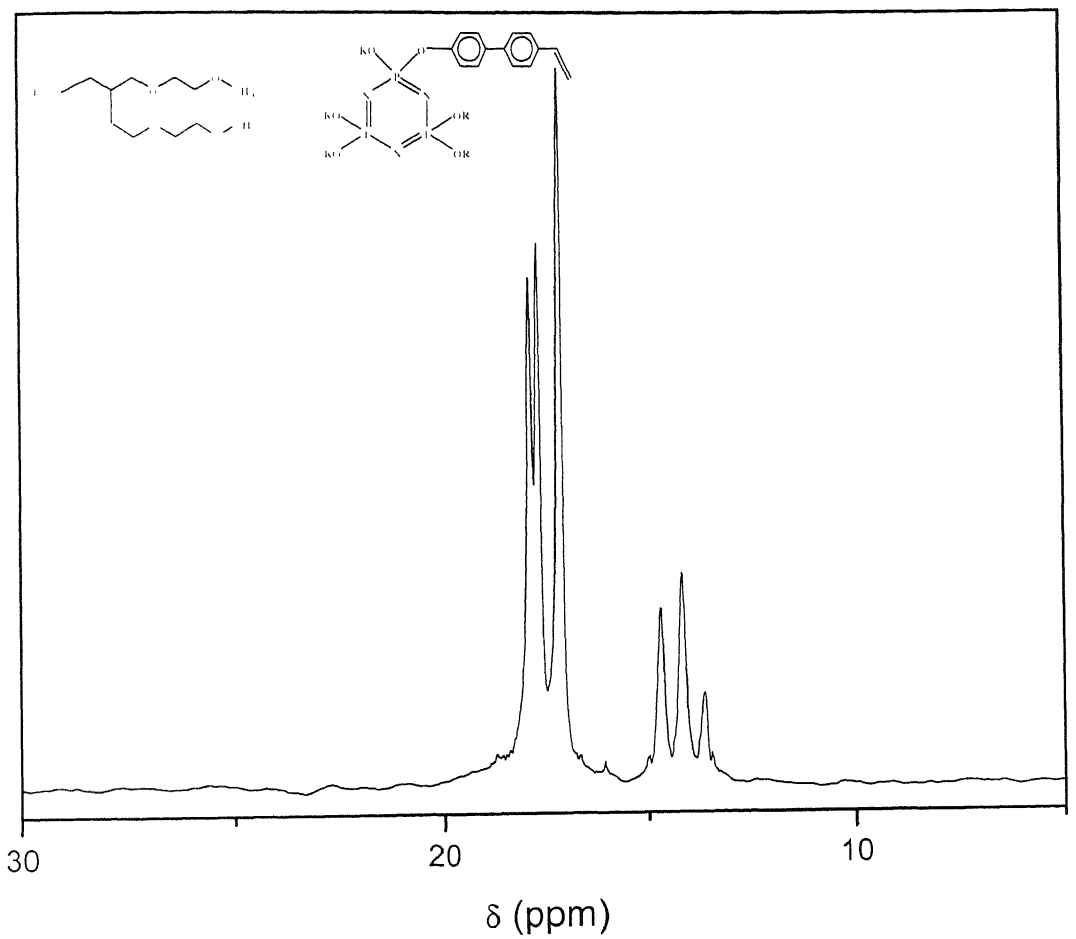

Figure 2.8 ^{31}P NMR spectrum of POMEE

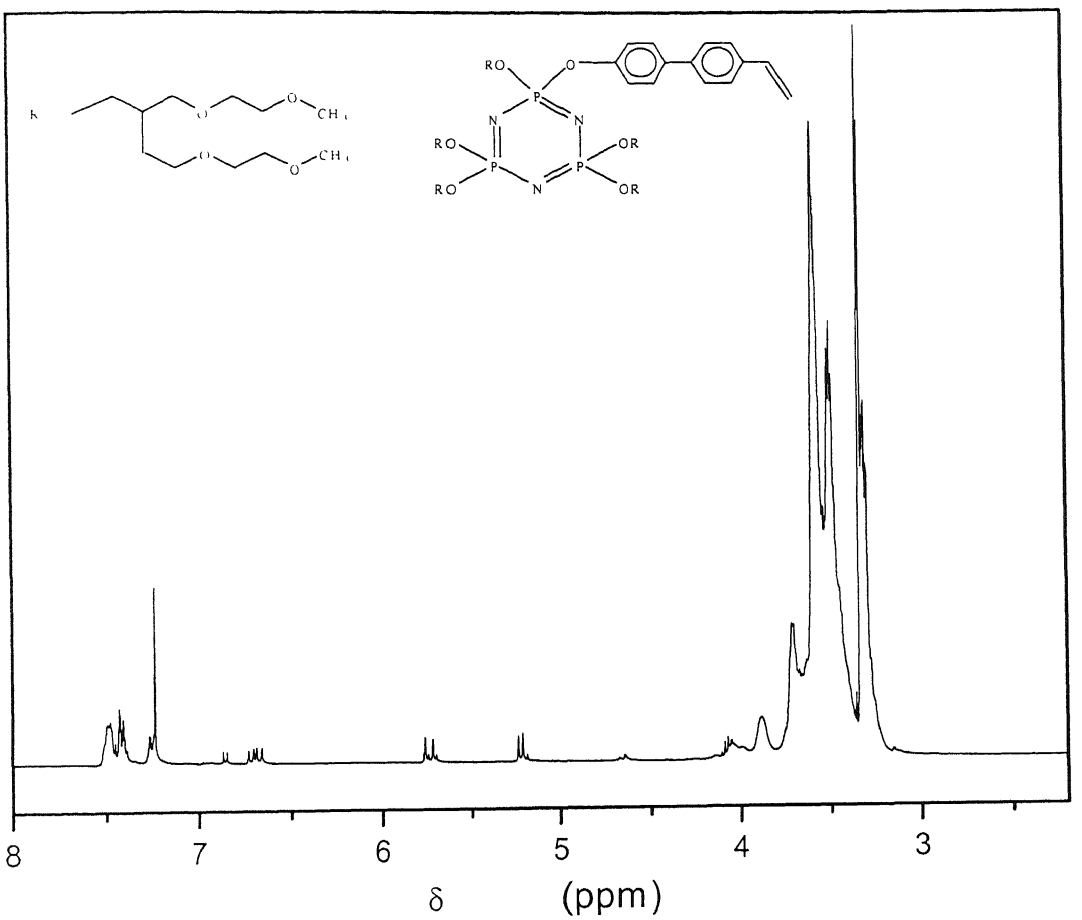

Figure 2.9 ^{1}H NMR spectrum of POMEE

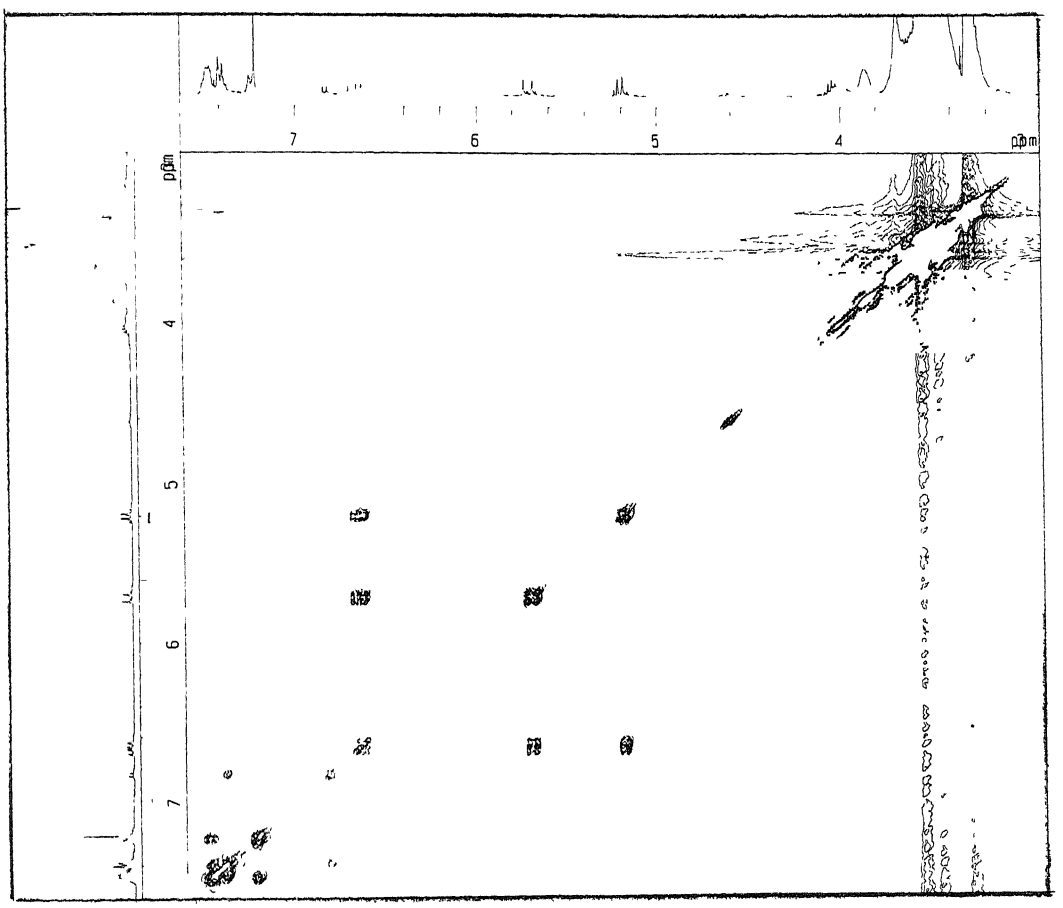

Figure 2.10 2D ^{1}H-^{1}H COSY NMR spectrum of POMEE

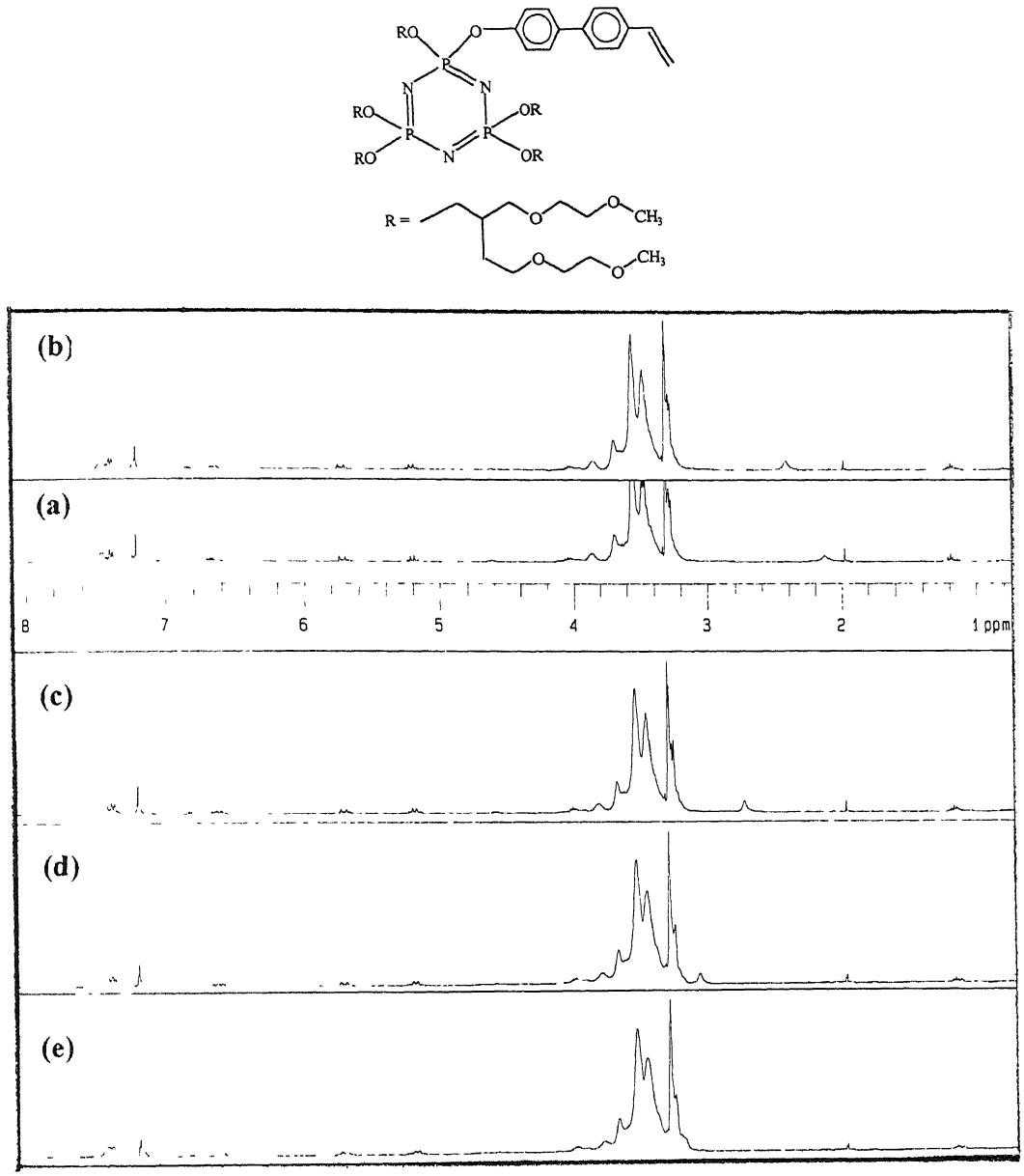

Figure 2.11 Comparison of the ^{1}H NMR spectra of POMEE recorded at (a) 25 °C (b) 0 °C (c) –20 °C (d) –40 °C (e) –50 °C

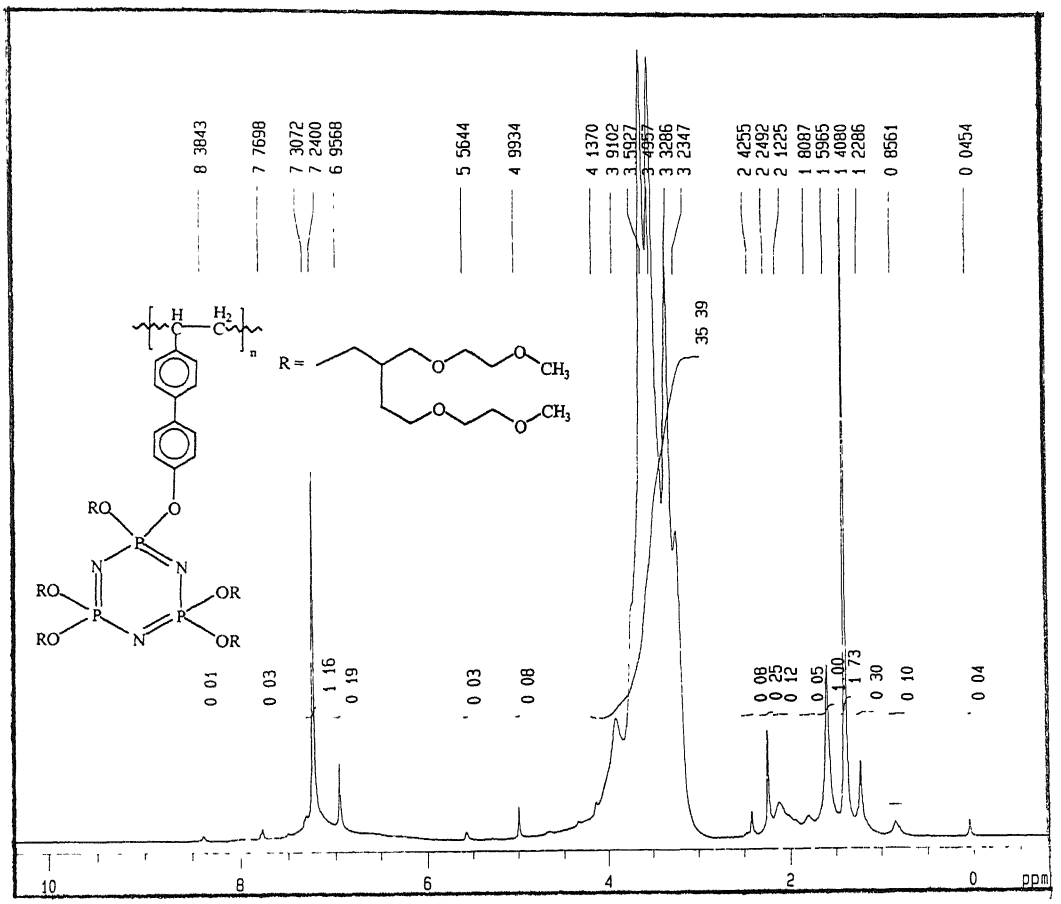

Figure 2.12 ^{1}H NMR spectrum of PPOMEE

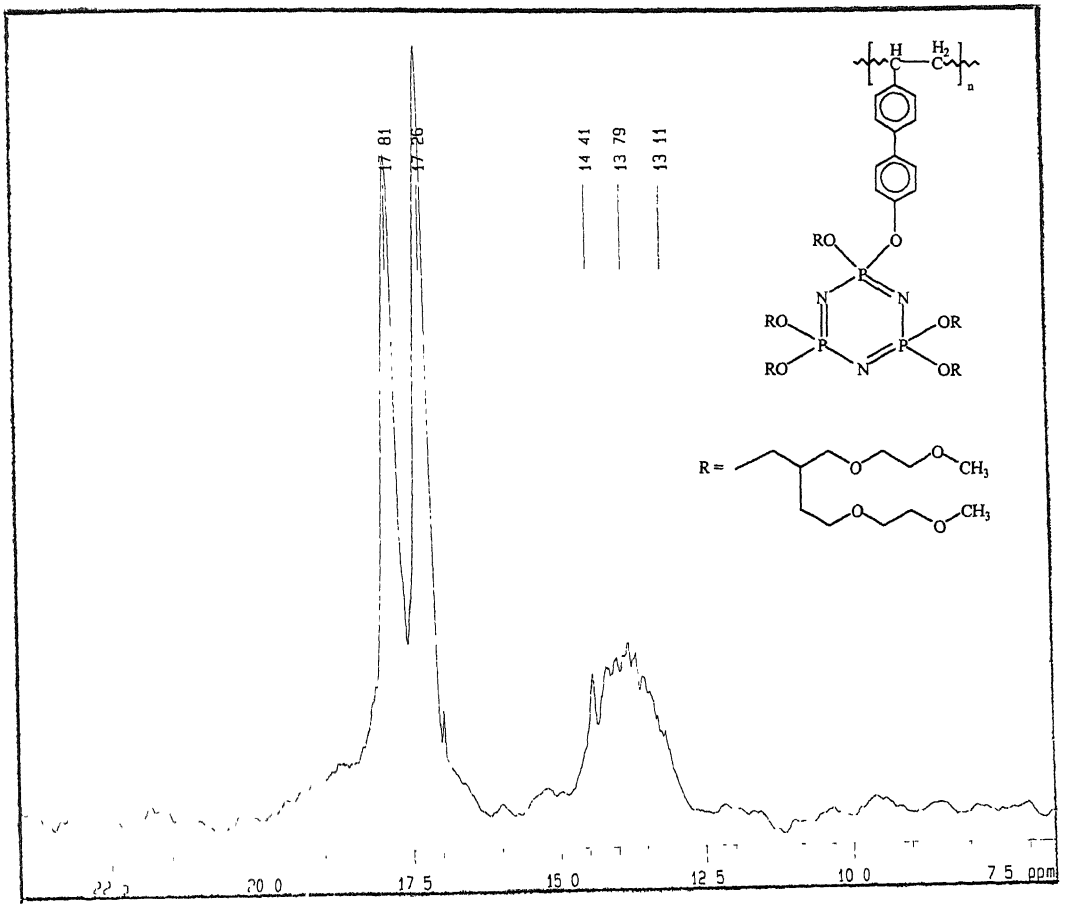

Figure 2.13 ^{31}P NMR spectrum of PPOMEE

Synthesis, Characterization and Ionic Conductivity studies of poly(2-[(4′-vinyl-4-biphenylyl)oxy]-2,4,4,6,6-pentakis[2-(2-methoxy ethoxy)ethoxy]cyclotriphosphazene):NaI complexes

A polymer electrolyte can be prepared in general by two methods. One is the conventional salt-in-polymer method, where calculated quantities of a salt and the polymer are dissolved in a common solvent such as acetonitrile, methanol or THF followed by a slow removal of the solvent in vacuum. The other method is the polymer-in-salt method reported by Angell and coworkers[68], in which salts are mixed with small amounts of the polymer to afford rubbery materials with low glass transition temperature The advantage of the latter is that the polymer electrolytes show high electrochemical stability Although other methods such as intimate grinding or mechanical mixing in the solid state have been employed[69], by far the most common method used for the preparation of polymer electrolytes is the salt-in-polymer method.

3.1 Materials used

Sodium Iodide (Aldrich, USA), ethanol (S. D. fine, India), PPMEE (as synthesized) Sodium Iodide was dried in a vacuum oven at 50 °C before use. Ethanol was dried as reported in literature[65]

3.2 Measurements

The polymer electrolytes prepared were characterized using X-Ray diffraction (XRD), infrared (IR) and impedance spectroscopy. The XRD patterns were recorded using Rich Siefert Iso-Debyeflex 200 2D counter diffractometer employing a filtered CuK-α radiation (λ = 1 542 Å) IR spectra were recorded on a Bruker Vector 200 series model FT- IR spectrophotometer. Electrical measurements were made using Hewlett Packard HP-4274A multi-frequency LCR meter. An indigenously configured MATLAB™ code was used to fit the impedance data.

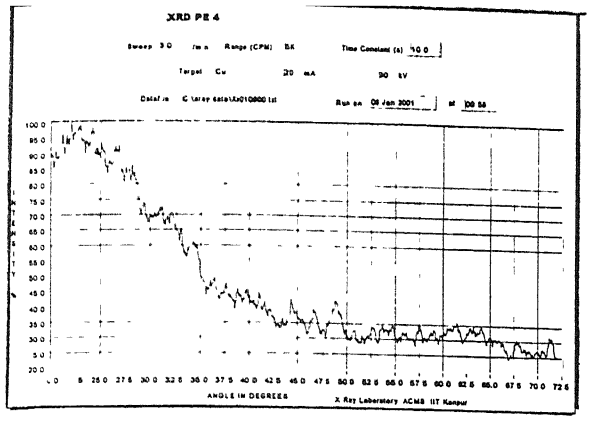

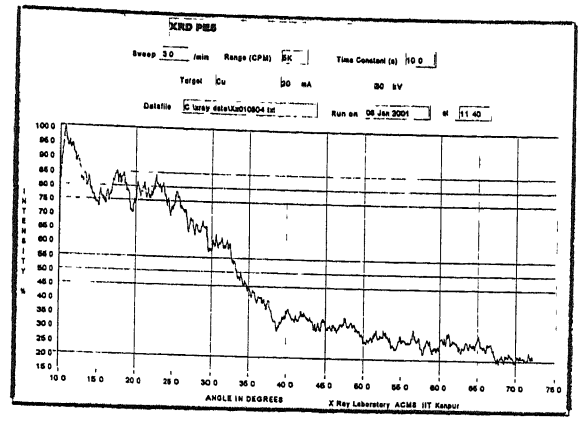

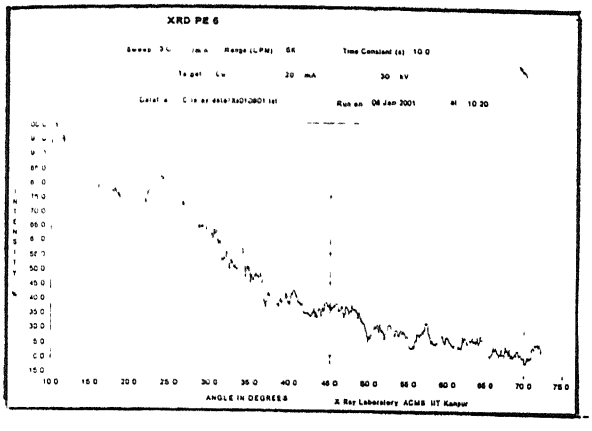

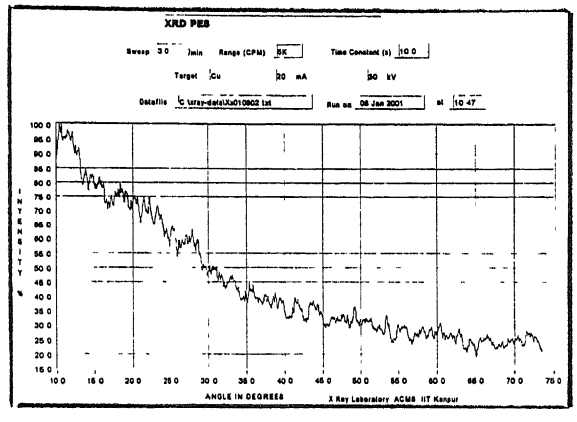

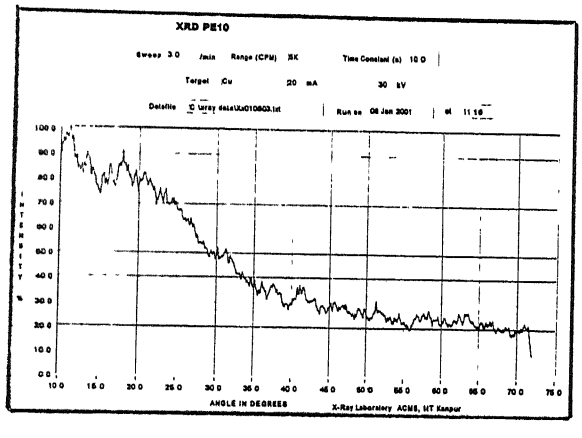

Figure 3.1 XRD patterns of PPMEE$_x$:NaI complexes

changes have been observed The peak position corresponding to the C-O-C stretching (1112 cm^{-1}) in the case of pure PPMEE, is shifted by about 20 - 35 cm^{-1} in the polymer electrolytes to around ~1080 cm^{-1}, suggesting that there is a weak interaction possibly

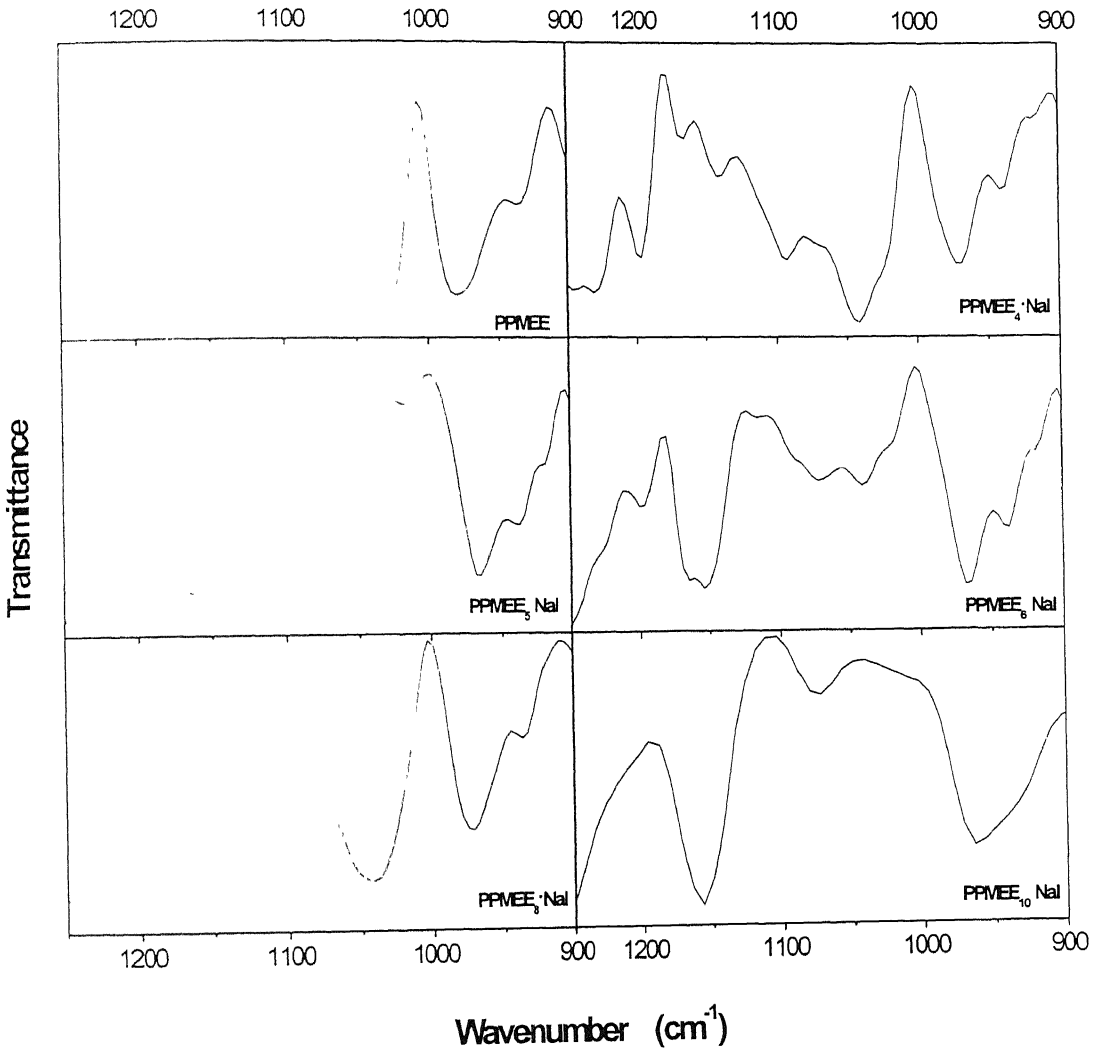

Figure 3. 2 IR spectra of PPMEE and its various complexes with NaI

between the ether oxygen of the side-chains in the polymer and the alkali metal ion of the salt used for complexation. Thus, the compositions of the polymer - salt complexes

can also be expressed as O Na ratios. The prominent peak positions obtained for the various salt complexes are listed in **Table 3.1**.

Table. 3.1. C-O-C stretching frequencies for the $PPMEE_x$:NaI complexes

O:Na ratio	C-O-C stretching frequency $\nu_{C\text{-}O\text{-}C}$ (cm^{-1})
0 (pure)	1112 (s)
4	1091(m)
5	1075(m)
6	1072(m)
8	1086(m)
10	1080(m)

(s) = strong, (m) = medium in terms of intensity of the band

3.4.3 Electrical measurements

3.4.3.1 Ionic conductivity studies on $PPMEE_x$: NaI complexes

Various compositions of $PPMEE_x \cdot NaI$ (x = 4, 5, 6, 8 & 10) were prepared by varying the O Na ratios The dried samples supported by teflon rings were used for conductivity measurements. Each sample was heated upto 60 °C and cooled to room temperature so as to resolidify it from the melt and form a homogeneous composition inside the teflon ring The role of the teflon ring was to maintain a definite geometry (cell constant) of the electrolyte sample The measurements were carried out over a frequency range of 100 Hz to 100 kHz To avoid cell polarization, a.c impedance analysis was carried out using silver electrodes. A block diagram of the sample holder used is given in **Figure 3.3** In view of the strong frequency dependent impedance of the sample, d.c conductivity of each composition between temperature range of 20 to 50 °C in steps of 2 to 3 °C was measured Measurements were taken both during the heating and the cooling cycle to check for the reproducibility and hysteresis effects if any. **Figures 3.4** and **3.5** show the representative complex impedance spectra of some metal-salt complexes at

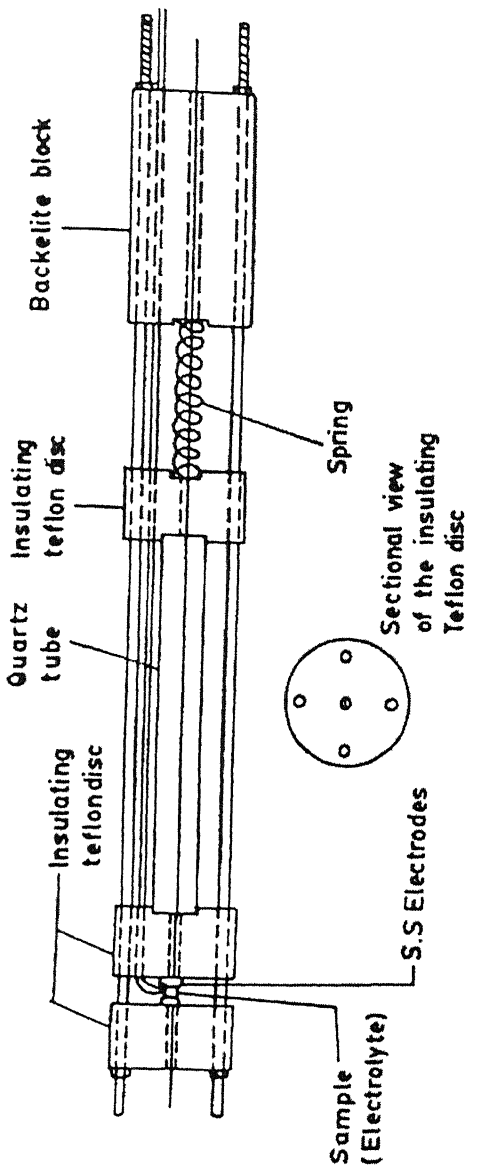

Figure 3.3 Block diagram of the sample holder used in electrical measurements

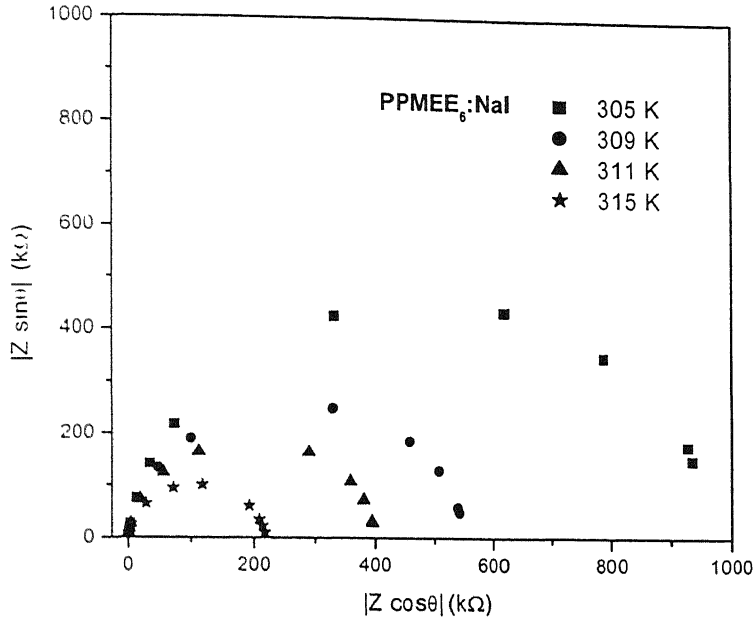

Figure 3.4 Complex impedance spectra of $PPMEE_6$:NaI complex at different temperatures

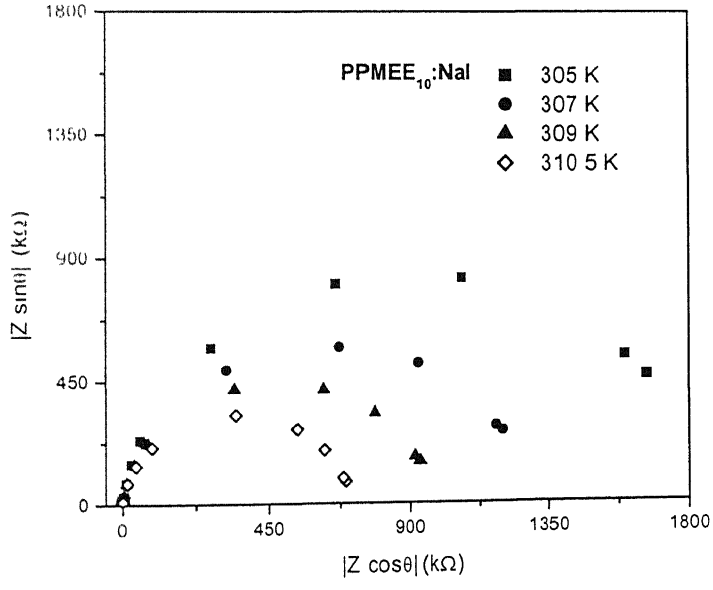

Figure 3. 5 Complex impedance spectra of $PPMEE_{10}$:NaI complex

different temperatures From the complex impedance spectra, the d.c resistance, R_{dc}, of the samples at different temperatures were obtained and the conductivity computed according to the equation,

$$\sigma_{dc} = \frac{l}{AR_{dc}} \qquad (3.1)$$

where l is the thickness and A is the area of cross-section of the sample respectively The d c conductivity of the pure polymer could not be determined using this technique due to the flowing nature of the polymer The object of the ionic conductivity studies is mainly to study the variation of conductivity with temperature and composition.

Ionic conductivity versus composition studies:

Figures 3.6 (a) and **(b)** show the log σ_{dc} vs. mole fraction of NaI and logσ_{dc} vs O Na ratios plots for the PPMEE$_x$. NaI complexes at five different temperatures The plot reveals that this system belongs to category II of the polymer electrolytes discussed in **Chapter 1**. As we increase the concentration of the salt the O.Na ratio decreases as there will be more number of Na^+ ions present for the available O in the polymer. The conductivity increases initially as the salt concentration increases, attains a maximum at O Na = 6 (σ_{dc} 3.42 x 10^{-6} Ω^{-1} cm^{-1} at 47 °C) and then starts decreasing with further addition of the salt This behaviour can be explained as follows The conductivity is related to the number of charge carriers by the equation,

$$\sigma_{dc} = \Sigma n_i q_i \mu_i \qquad (3.2)$$

where n_i, q_i and μ_i are the number of charge carriers per unit volume, the charge and the mobility of the charge carriers respectively. Hence the increase in conductivity in the initial stage when the salt concentration is increased may be due to the increase in the number of charge carriers The fall in the conductivity after attaining a maximum value at a particular concentration of the salt may possibly be because the salt acts as a weak cross-linker at higher concentrations raising the value of T_g. One then expects the conductivity to drop with further increase in concentration.

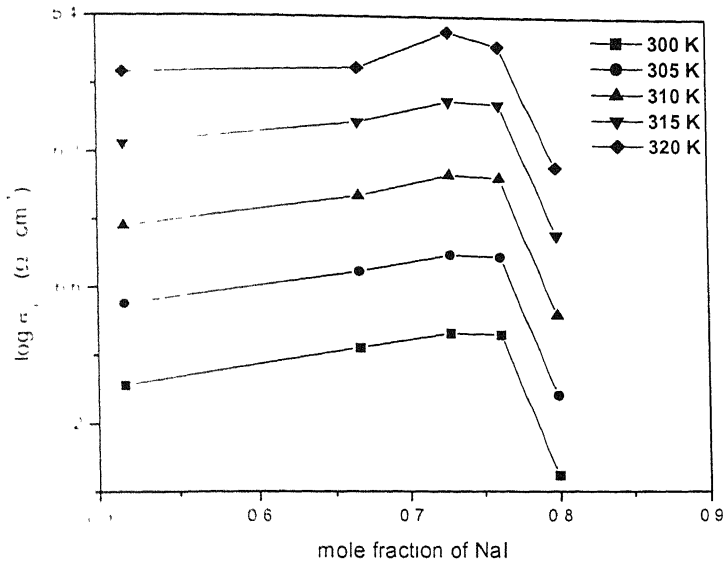

Figure 3.6 (a) Variation of conductivity with composition for $PPMEE_x$:NaI

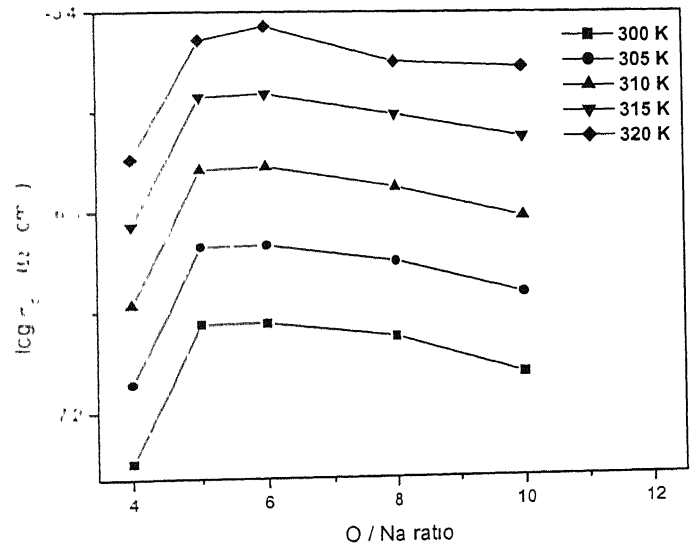

Figure 3.6 (b) Variation of conductivity with O:Na ratios for $PPMEE_x$:NaI

Ionic conductivity versus temperature studies:

The electrical conductivity versus temperature behaviour for the polymer-salt complexes is generally described either by an Arrhenius equation,

$$\sigma = \sigma_o \exp\left(\frac{-E}{kT}\right) \qquad (3.3)$$

where σ_o is a constant and E is the activation energy required for ion-hopping, or by the Vogel-Tamman-Fulcher (V-T-F) equation,

$$\sigma = A' T^{1/2} \exp\left(\frac{-E_a/k}{T - T_o}\right) \qquad (3.4)$$

where E_a is the apparent activation energy which is very different from E in Eq (3) T_o is a temperature close to the ideal glass transition temperature and A' is a constant proportional to the carrier concentration The value of T_o is obtained from the V-T-F plot **Figure 3.7** shows the Arrhenius plots of log σ_{dc} vs 1000 / T for the entire series of polymer salt complexes prepared in this work The plot indicates clearly that there is an increase in the conductivity with increase in the temperature. The maximum conductivity recorded is for the salt-complex with O:Na = 6 (5.36 x 10^{-6} Ω^{-1} cm^{-1} at 51 °C) The activation energies calculated from the Arrhenius plots for the various complexes are given in **Table 3.2** These values of the energy barrier for ion transport are low compared to the reported values[5] for PEO-NaI complexes ($E \sim 1.4$ eV). The lower activation energy for these complexes may be due to the completely amorphous nature of the samples A plot of the activation energy values vs. composition is given in **Figure 3.8.**

The log σ_{dc} vs 1000 / T plots (**Figure 3.7**) show a slight curvature (non-Arrhenius behaviour) due to the amorphous nature of the materials. Hence conductivity data were also fitted to the V-T-F equation by plotting $\{ \ln[\sigma T^{1/2}/ A']\}^{-1}$ vs T (**Figure 3.9**). Since the constant A' is proportional to the carrier concentration the mole fraction of the salt added is taken as A' in each case As evident from **Figure 3.9**, the V-T-F plots are quite linear for all the complexes. These linear graphs also yield the values of T_o in addition to apparent activation energy, E_a, which are listed in **Table 3.3** It is noted that the temperature T_o of Eq. 3.4, a temperature close to the glass transition temperature, T_g depends on the concentration of the salt in the complex Due to the non-availability of the

DSC instrument, which is used to measure T_g values of T_g could not be obtained and compared with T_o. But the observed variation of T_o may be correlated to the variation of conductivity with composition (**Figure 3.6 a & b**) T_o is maximum for the composition with O:Na ratio of 6, for which conductivity is maximum and the variation is also similar with T increasing with salt concentration, attaining a maximum and then decreasing The apparent activation energy values are also found to be dependent on the salt concentration (**Figure 3. 11**) The complex with O:Na = 6, which has high conductivity, has the lowest value of apparent activation energy, E_a (0 07 eV) (**Figure. 3.10**).

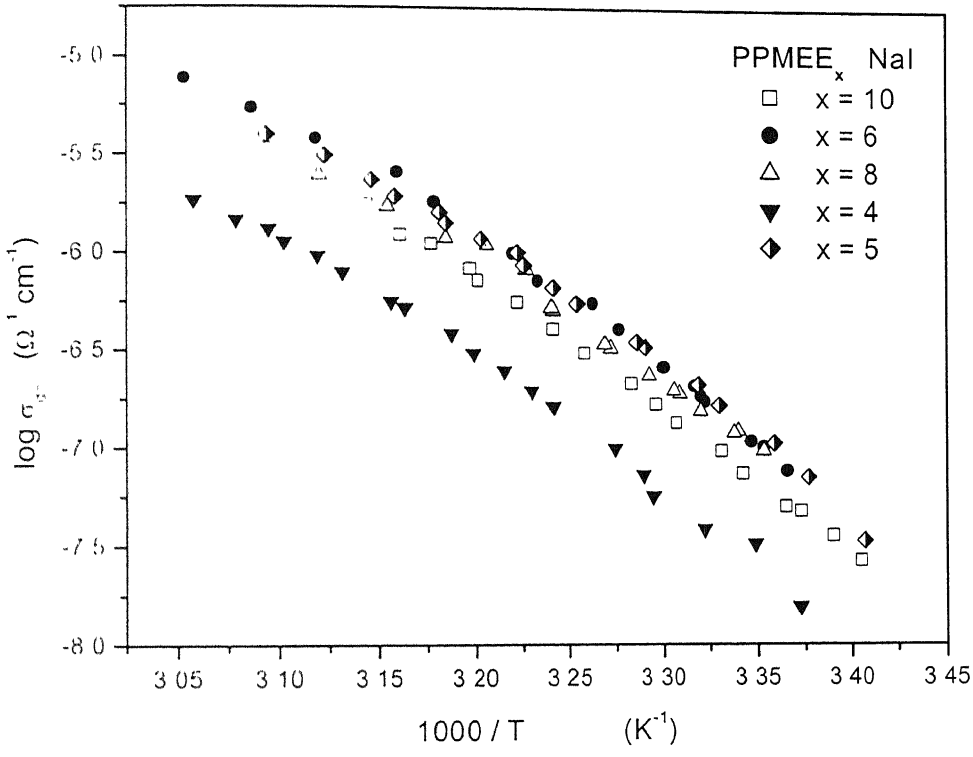

Figure 3.7 The log σ_{dc} vs. 1000 /T plot for various PPMEE$_x$: NaI complexes.

Table 3. 2 Activation energy values obtained from Arrhenius plots (log σ_{dc} vs. 1000/T)

Composition (O Na ratio)	Activation energy, E (eV)
4	0.57
5	0 56
6	0.55
8	0 57
10	0 58

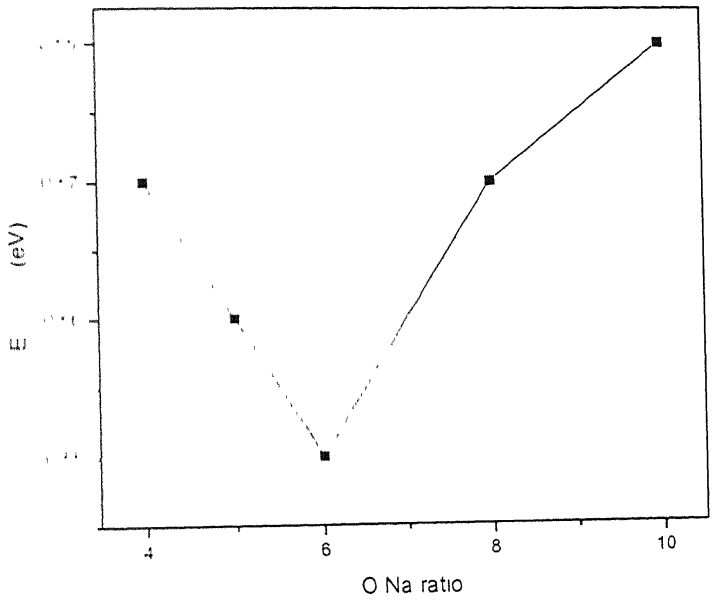

Figure 3. 8 Plot of Activation energy values (obtained from Arrhenius plots) vs. O:Na ratios of various PPMEE$_x$: NaI complexes

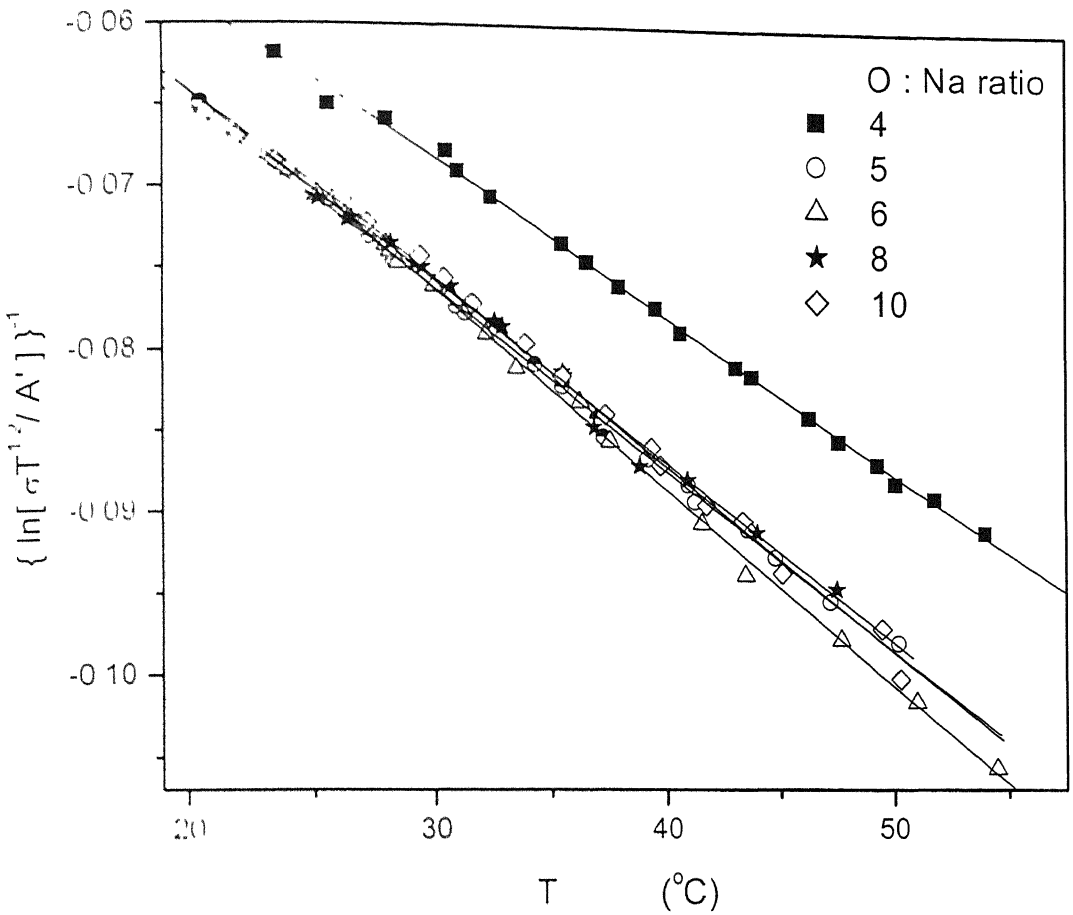

Figure 3. 9 V-T-F plots for $PPMEE_x$: NaI complexes

Table 3. 3 The best fit parameters obtained from V-T-F plots for $PPMEE_x$: NaI complexes

Composition (O:Na ratio)	A′ (Ω^{-1} cm^{-1} $K^{1/2}$)	Apparent Activation energy E_a (eV)	T_o (K)
4	0.80	0 09	232 4
5	0.76	0 078	234.6
6	0.73	0 071	240 2
8	0.67	0.078	234 8
10	0.52	0 075	237 4

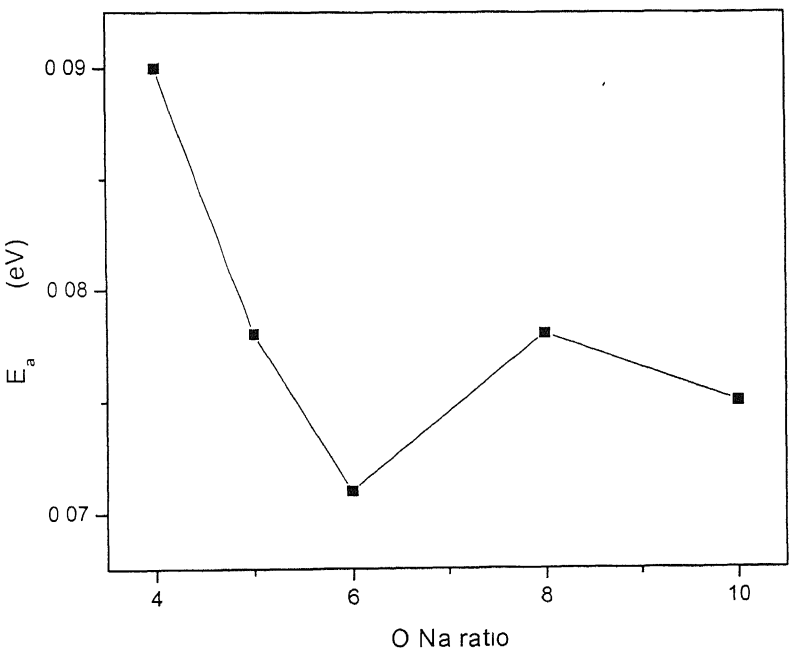

Figure 3.10 Variation of Apparent Activation energy with composition for $PPMEE_x$:NaI complexes

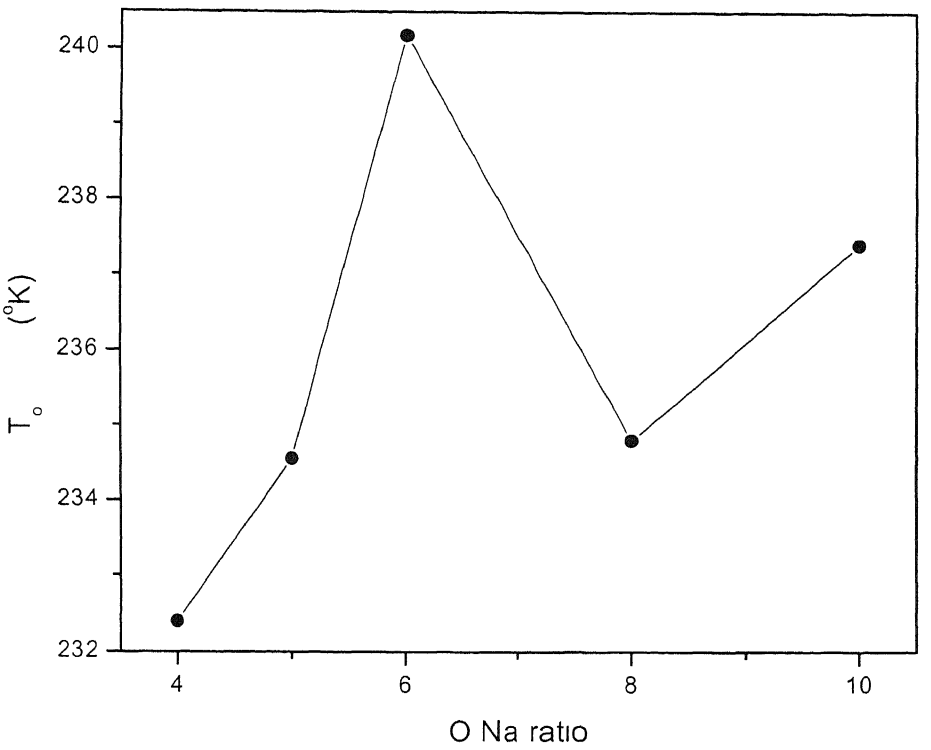

Figure 3.11 Variation of T_0 with composition for $PPMEE_x$: NaI complexes

3.4.3.2 Electrical Relaxation Studies

The studies on the frequency dependence of conductivity and the dielectric constant are useful in discriminating between the various ion transport mechanisms in polymer electrolytes[9, 70].

The complex admittance (Y^*) is the inverse of complex impedance and is related to the resistance (R_b) and the capacitance (C_p) of the sample (in parallel mode) by the relations,

$$Y^* = \frac{1}{Z^*} = Y\cos\theta + jY\sin\theta \qquad (3\ 5)$$

$$Y^* = \frac{1}{R_b} + j\omega C_p \qquad (3.6)$$

Thus we have,

$$\frac{1}{R_b} = Y\cos\theta \qquad (3.7)$$

and $$\omega C_p = Y\sin\theta \qquad (3.8)$$

The complex permittivity, ε^* is given by,

$$\varepsilon^* = \varepsilon' - j\varepsilon'' = \frac{Y^*}{j\omega C_o} \qquad (3.9)$$

The real (ε') and the imaginary (ε'') part of the complex permittivity, ε^* are given by,

$$\varepsilon' = \frac{C_p}{C_o} = \frac{Y\sin\theta}{\omega C_o} \qquad (3.10)$$

and $$\varepsilon'' = \frac{1}{\omega C_o R_p} = \frac{Y\cos\theta}{\omega C_o} \qquad (3.11)$$

where $C_o = \varepsilon_o A/d$ is the capacitance of the cell in vacuum without the sample ε_o is the permittivity of vacuum and A and d are the area of cross-section and separation between the electrodes respectively. Thus from the measured impedance data, ε' and ε'' can be calculated

The frequency dependence of the impedance data can be clearly observed when the imaginary part of the complex impedance is plotted against log ($\omega/2\pi$) Such plots indicate the relaxation processes present that are responsible for conductivity, etc. Curves with a maximum at certain frequencies that are characteristic of the relaxation processes are obtained in the plot **Figure 3.12** shows a representative plot of such type for $PPMEE_6$·NaI at four different temperatures. The plot reveals that the maximum (relaxation frequency, ω_{max}) shifts to the higher frequencies as temperature increases

ω_{max} values at different temperatures were also determined for other complexes in a similar manner. For any thermally activated process the relaxation frequency is given by the relation,

$$\omega_{max} = \omega_o \exp\left(-\frac{E}{kT}\right) \qquad (3.12)$$

where ω_o is a constant (inverse of relaxation time, τ_0) and E is the activation energy associated with the process A plot of log (ω_{max} / 2π) vs. $1/T$ (**Figure 3.13**) yields the

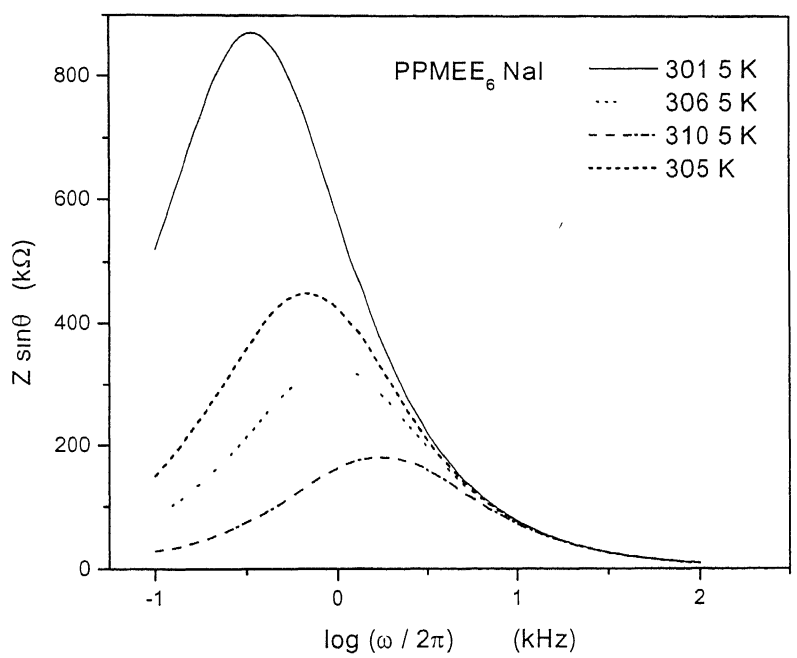

Figure 3. 12 Frequency dependence of the imaginary part of impedance for PPMEE$_6$:NaI complex

activation energy values **Table 3.4** lists the activation energy values and relaxation times obtained from the plot for various complexes prepared. These activation energy values are approximately equal to those obtained from the plot of log σ_{dc} vs. 1000 / T. This indicates that the relaxation occurring at ω_{max} is also responsible for the conduction

process. The small discrepancy (±0.02 eV) in the two activation energy values (**Table 3.4**) is well within the experimental error The good agreement between the activation energies obtained $\sigma(T)$ and $\omega_{max}(T)$ clearly suggest that a single thermally activated mechanism is responsible for both ionic conduction and dielectric relaxation. The values of the relaxation times ($\tau = 2\pi/\omega_{max}$) of the complexes prepared also vary in agreement

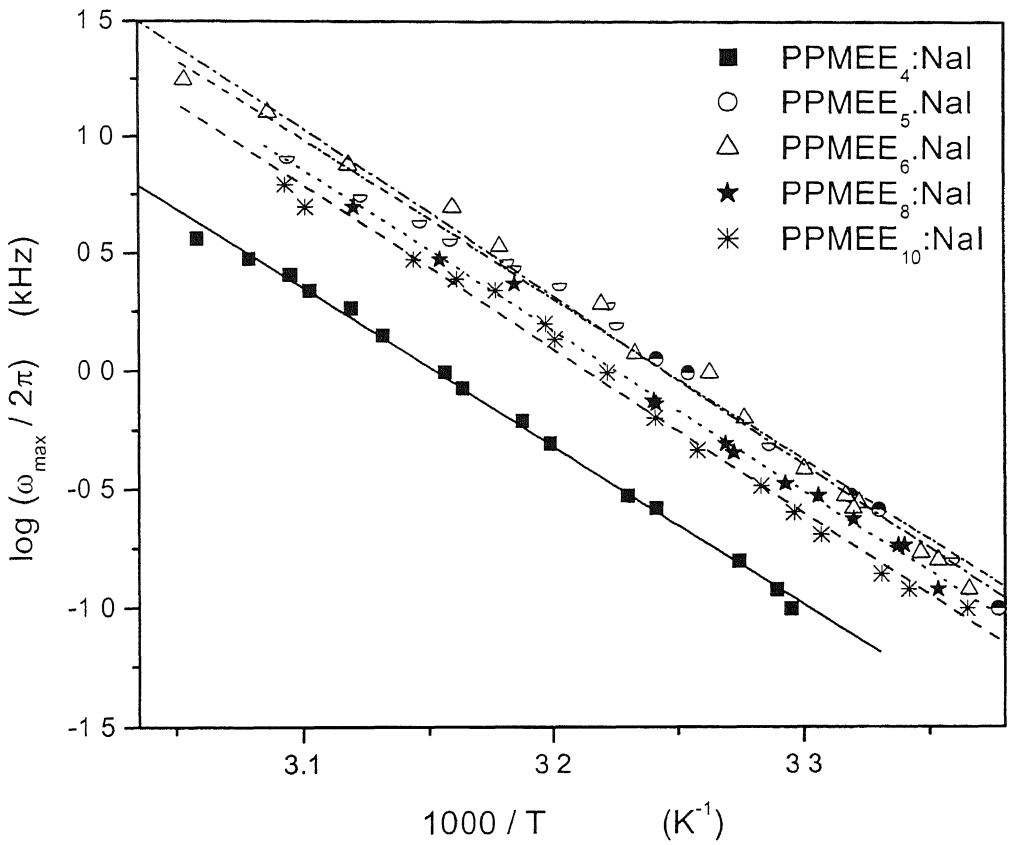

Figure. 3. 13 Variation of the relaxation frequency with temperature

with the composition behaviour indicating that $PPMEE_6$ NaI has very low relaxation time when compared to other complexes. The relaxation times for the complexes at 44 °C are given in **Table 3.4**.

Table 3. 4 Activation energy values obtained from log (ω_{max}/ 2π) vs. 1000/T plot.

Composition (O Na ratio)	Activation energy for relaxation (eV)	Activation energy for conduction (eV)	Relaxation time, τ at 44°C (seconds)
4	0 58	0 57	0 98
5	0.59	0 56	0 23
6	0.57	0.55	0 21
8	0.59	0 57	0 30
10	0.60	0 58	0 37

Dielectric Studies:

As pointed out earlier, the same impedance data (Z, θ) can be used to calculate the dielectric constant as well (Eqs 3.10 - 11). All the polymer electrolytes studied showed similar type of variations of the dielectric constant values with frequency and temperature. **Figure 3. 14** shows the results of one polymer electrolyte ($PPMEE_6$·NaI) studied in this work It is observed that the dielectric constant is strongly dependent on both the frequency and temperature. The high value of ε' at relatively low frequencies may be attributed to interfacial polarization, which tends to ease out as frequency increases and hence ε' decreases rapidly at higher frequencies. The presence of interfacial polarization can also account for the higher values of ε' at higher temperatures and lower frequencies. Since the ionic conductivity or mobility is higher at higher temperatures, this would essentially lead to fast arrival of ions at the interfaces and thus more accumulation of charges at the interface

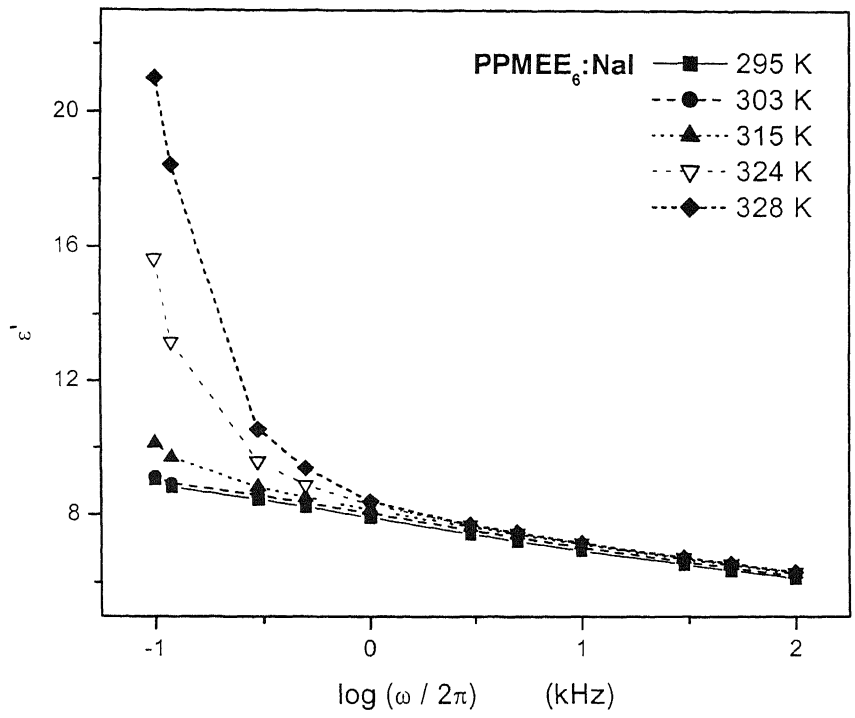

Figure 3 .14 Dielectric constant as a function of frequency for $PPMEE_6$:NaI at five different temperatures

Thus based on the observations and interpretations a qualitative picture of the ion transport in PPMEE$_x$ NaI is given below.

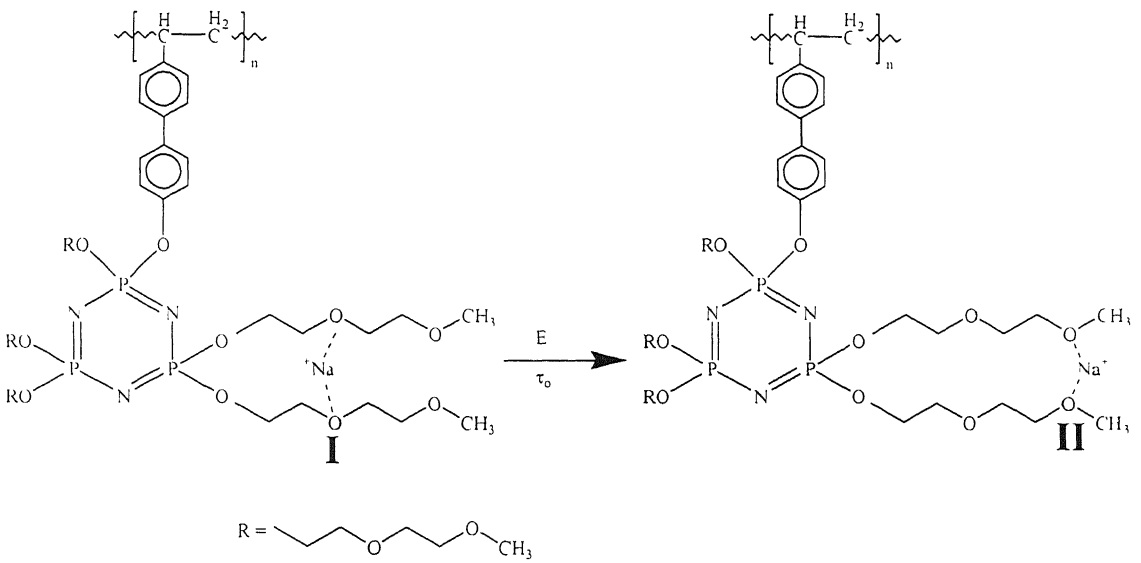

The Na^+ ion moves from position **I** to position **II** when the energy supplied is equal to the activation energy of the hopping process in a time τ, which is the relaxation time The hopping occurs due to the conformational changes in the oxyethylene segments which occur during relaxation

Chapter 4

Conclusions and Future scope

The results obtained from the present study can be summarized as follows

The polymer PPMEE has been synthesized, characterized using various available techniques and the results reported. The polymer has been complexed with sodium iodide and several studies have been carried out on the complexes The electrical conductivity of the polymer-salt complex is found to increase with increasing temperature and the electrolytes show a better conductivity than the PEO analogues The Arrhenius activation energies obtained from the log σ_{dc} vs. $1000/T$ and log (ω_{max} /2π) vs $1000/T$ plots are in agreement indicating that the same mechanism is responsible for both ionic conduction and dielectric behaviour The activation energy required for the relaxation responsible for conduction is also lower than that for PEO based complexes The conductivity values obtained were also fitted with the V-T-F equation, since the Arrhenius plots showed a slight curvature. The V-T-F plots were found to be reasonably linear from which the apparent activation energy values calculated $PPMEE_6$ NaI complex, which showed the highest conductivity, was also found to have the lowest apparent activation energy XRD and IR studies prove complete complexation of the salt with the polymer The complexes prepared are completely amorphous which is a main requirement for a polymer electrolyte to suit practical applications The polymer-salt complexes have very low dielectric constant values. All these characteristics make it a potential candidate for use in electrolytic applications.

A new polymer with branched oxyethylene side-chains, PPOMEE has been prepared This polymer has been characterized using the various NMR techniques

available. Low temperature NMR studies prove that the motions of the branched segments get restricted with the decrease of temperature Due to the diffused contours obtained in the COSY spectrum the peaks could not be assigned to each $-CH_2CH_2O-$ group. However from the application point of view this polymer can act as a good host for metal salts due to the large number of basic sites present

The new polymer, PPOMEE is a gel-like material Due to the presence of more number of basic sites, it can be complexed with more cations and hence can show higher conductivity Solid state batteries could be devised based on these systems and the battery characteristics may be studied

References

1 Tubandt, Lorenz *Z Physik Chem* **1914**, *87*, 513.

2. Chandra, S *Super Ionic Solids* **1981**, North Holland Publishing Company

3 Johnson, R T Jr , Morosin, B ; Knotek, M L ,Biefeld, R M *Phys Letts.* **1975**, *54A*, 403

4 Karvamoto, Y , Nagura, N , Tsuchihashi, S. *J Am Ceram Soc* **1974**, *57*, 489

5 Fenton, D E , Parker, J M., Wright, P V *Polymer* **1973**, *14*, 589

6 Armand, M B , Chabagno, J M., Duclot, M J. *Fast Ion Transport in Solids*, Vashishta, P , Mundy, J N , Shenoy, G K Eds North Holland, Amsterdam **1979**, pg131

7 Ratner, M A , Shriver, D F *Chem Rev* **1988**, *88*, 109

8 Berthier, C , Gorecki, W , Minier, M , Armand, M B ; Chabagno, J M , Rigaud, P *Solid State Ionics* **1983**, *11*, 91

9 Ansari, S M , Brodwin, M , Papke, B L ; Shriver, D. F *Solid State Ionics* **1986**, *17*, 101.

10. Watanabe, M , Ogata, N.; *In Polymer Electrolyte Reviews*, Elsevier, London **1987**

11 Nicholas, C V , Wilson, D J , Booth, C , Giles, J R M. *Abstracts First International Symposium on Polymer Electrolytes*, St Andrews, Scotland **1987**, pg 273

12 Manoravi, P ; Selvaraj, I. I , Chandrasekhar, V., Shahi, K *Polymer.* **1993**, *34*, 1339

13 Harris, C S , Shriver, D F.; Ratner, M A *Macromolecules.* **1986**, *19*, 987

14 Blonsky, P M ; Shriver, D F , Austin, P ; Allcock, H R. *J Am Chem Soc* **1984**, *106*, 6854

15 Blonsky, P. M , Shriver, D F.; Austin, P , Allcock, H R *Solid State Ionics* **1986**, *18/19*, 258

16 Hall, P G., Davies, G. R.; McIntyre, J E., Ward, I M., Bannister, D J., Le Braq, K M F *Polym Commun.* **1986**, *27*, 98.

17 Xia, D W , Soltz, D ; Smid, J *Solid State Ionics* **1984**, *14*, 221

18. Cowie, J M G., Ferguson, R *J Polym Sci Polym Phys Ed* **1985**, *23*, 2181.

19 Selvaraj, I. I.; Chaklanobis, S.; Chandrasekhar, V. *J Polym Sci Polym Chem Ed* **1993**, *31*, 2643

20 Selvaraj, I. I., Chaklanobis, S , Chandrasekhar, V. *J Electrochem Soc* **1995**, *142*, 366.

21 Selvaraj, I I , Chaklanobis, S ; Manoravi, P , Chandrasekhar, V *Polymer* **1995**, *36*, 2603

22 Mark, J E , Allcock, H. R , West, R *Inorganic Polymers* Prentice Hall, New Jersey, USA **1992**

23 Cheradame, H *IUPAC Macromolecules*, Benoit, H ; Rempp, P Eds Pergamon Press, New York **1982**, pg 251.

24 Killis, A , LeNest, J. F ; Cheradame, H *Makromol Chem Rapid Commun* **1980**, *1*, 5953

25 Killis, A , LeNest, J F , Gandini, A , Cheradame, H., Cohen Addad, J. P. *Solid State Ionics* **1984**, *14*, 231.

26 Tonge, J S , Shriver, D F *J Electrochem. Soc* **1987**, *134*, 269

27 Spindler, R , Shriver, D F. *Macromolecules* **1988**, *21*, 648.

28 MacCallum, J R , Smith, M J , Vincent, C A. *Solid State Ionics* **1984**, *11*, 307

29 Killis, A , LeNest, J F *Macromolecules* **1984**, *17*, 63.

30 Watanabe, M , Itoh, M , Sanui, K., Ogata, N *Macromolecules* **1987**, *20*, 569

31 LeNest, J F , Cheradame, H , Gandini, A *Solid State Ionics*. **1988**, *28 – 30*, 1032

32 Lee, Y L., Crist, B *J Appl Phys* **1986**, *60*, 2683.

33 Albensson, I , Jacobsson, P. *Solid State Ionics*. **1992**, *53 – 56*, 1059

34 Mendolia, M S , Farrington, G C *Solid State Ionics* **1992**, *9/10*, 1125

35 Cai, H , Hu, R *Solid State Ionics*. **1992**, *52*, 333

36 Chiang, C K , Davis, G. T *Solid State Ionics* **1983**, *9/10*, 1121

37. Dupon, R , Papke, B L *J Am Chem Soc*. **1982**, *104*, 247

38 Selvaraj, I. I ; Chaklanobis, S , Chandrasekhar, V *J Electrochem Soc* **1995**, *142*, 3434

39 Ratner, M A *In Polymer Electrolyte Reviews*. MacCallum, J. R , Vincent, C A Eds Vol I, Elsevier. **1987**, pg 173.

40 Kobayashi, N ; Uchiyama, M *J Phys Chem* **1985**, *89*, 987.

41 Doolittle, A. K.; Doolittle, D. B *J Appl Phys* **1957**, *26*, 901.

42 Cohen, H. H , Turnbull, D. J. *J Chem Phys* **1959**, *31*, 1164.

43 Goldstein, M *J Phys Chem* **1973**, *77*, 667

44 William, M L , Landel, R. F , Ferry, J D *J Am Chem Soc* **1955**, *77*, 3701

45 Gibbs, J H , DiMarzio, E A *J Chem Phys.* **1958**, *28*, 373

46 Adam, G , Gibbs, J H *J Chem Phys* **1965**, *43*, 139

47 Druger, S D., Nitzan, A ; Ratner, M A *J. Chem Phys* **1983**, *79*, 3133

48 Druger, S D , Ratner, M A , Nitzan, A *Phys Rev B* **1985**, *31*, 3939

49 Iwanoto, R , Saito, Y ; Ishihara, H , Tadokoro, H *J Polym. Sci* (A-2) **1968**, *6*, 1509

50 Chatani, Y , Okamura, S *Polymer.* **1987**, *28*, 1815.

51 Lightfoot, P ; Nowinski, J L , Bruce, P G *J Am Chem Soc* **1994**, *166*, 7469

52 Davidson, W H. T *J Chem Soc* **1955**, 3270

53 Papke, B L , Ratner, M. A , Shriver, D. F. *J Phys Chem Solids.* **1981**, *42*, 493

54 Rhodes, C P., Frech, R *Solid State Ionics.* **2000**, *136/137*, 1131

55 Jin, J H , Hong, S U , Won, J , Kang, Y S *Macromolecules.* **2000**, *33*, 4932

56 Minier, M , Berthier, C., Gorecki, W. *Solid State Ionics* **1983**, *9/10*, 1125

57 Kulkarni, A R *Solid State Ionics* **2000**, *136/137*, 549

58 Gang, W , Roos, J *Solid State Ionics* **1992**, *53-56*, 1102

59 Allcock, H R , Napierala, M E , Olmeijer, D L , Best, S A , Merz Jr , K. M *Macromolecules.* **1999**, *32*, 732

60 Sonderegger, M , Roos, J *Solid State Ionics*. **1992**, *53/56*, 849

61 Lauenstein, A , Tegenfeldt, J , Kuhn, W *Macromolecules*. **1998**, *31*, 3886.

62 Bruce, P G *In Polymer Electrolyte Reviews*. MacCallum, J. R ; Vincent, C. A Eds Elsevier **1987**, pg 237

63 Inoue, K ; Nishikawa, Y., Tanigaki, T. *Macromolecules* **1991**, *24*, 3464.

64 Gupta, S *Ionic Transport in PEG-MX Polymeric Electrolytes*, Ph.D Thesis, IIT Kanpur **1994**, pg 31

65 Furniss, B S , Hannaford, A J ; Smith, P W , Tatchell, A R ***Vogel's*** *"Textbook of Practical Organic Chemistry"*, **1989**, 5th Ed. ELBS/Longman, UK

66 Tanigaki, T , Shirai, M ; Inoue, K. *Polymer J.* **1987**, *19*, 881.

67 Allcock, H. R , O' Connor, S. J M , Olmeijer, D. L., Napierala, M. E., Cameron, C G *Macromolecules* **1996**, *29*, 7544.

68 Angell, C A , Lin, C., Sanchez, E. *Nature*, **1993**, *362*, 137

69 Gray, F M , MacCallum, J. R., Vincent, C *Solid State Ionics* **1985**, *18/19*, 282

70 Fontanella, J J , Wilson, J J *Solid State Ionics* **1992**, *50*, 259